The icosahedron in inorganic chemistry

R. Bruce King
Department of Chemistry, University of Georgia, Athens, GA 30602 (USA)

Abstract

Icosahedral clusters of atoms are found in the following types of inorganic structures: (1) boron derivatives including the borane anion $B_{12}H_{12}^{2-}$ and its derivatives, the carboranes $C_2B_{10}H_{12}$, elemental boron, certain types of boron-rich metal borides such as Mg_2B_{14}, and boron carbide; (2) alkali metal gallides such as $RbGa_7$ and K_3Ga_{13}; (3) icosahedral quasicrystals containing large amounts of aluminum; (4) icosahedral transition metal carbonyl clusters of nickel and rhodium such as $Ni_9(AsPh)_3(CO)_{15}^{2-}$ and $Rh_{12}Sb(CO)_{27}^{3-}$; (5) icosahedral gold clusters such as $Au_{12}(Au)Cl_2(PMe_2Ph)_{10}^{3+}$. Analysis of the chemical bonding in these diverse icosahedral atomic clusters using graph-theory derived methods indicates delocalized bonding leading to relatively high chemical stabilities. In addition an icosahedron is found in the MO_{12} coordination polyhedron (M = Ce(IV), Th(IV), U(IV)) in the Silverton polyoxometalates $MMo_{12}O_{42}^{8-}$. The icosahedron is related to the cuboctahedron by a six-fold diamond-square process; cuboctahedra are found in a number of inorganic structures including the centered rhodium carbonyl cluster $Rh_{12}(Rh)(CO)_{24}H_3^{2-}$ and the Keggin polyoxometallates $XM_{12}O_{40}^{n-}$ ($n = 3$ to 7; M = Mo, W; X = B, Si, Ge, P, Fe^{III}, Co^{III}, Cu^{II}, etc.). The reducibility of Keggin polyoxometallates to molybdenum and tungsten 'blues' can be related to delocalization involving overlap of the d_{xy} orbitals on the twelve $(\mu_n\text{-O})_5MO$ vertices of a large cuboctahedron. The pure rotation point group of the icosahedron (*I*) is isomorphic to the group of even permutations of five objects (A_5) and is of group-theoretical significance in being the non-trivial simple group having the smallest number of operations.

1. Introduction

A key concept for the description of chemical structures is that of a polyhedron [1]. In three-dimensional space a polyhedron may be regarded as a set consisting of (zero-dimensional) points, namely the vertices; (one-dimensional) lines connecting some of the vertices, namely the edges; and (two-dimensional) surfaces formed by the edges, namely the faces. Polyhedra appear in structures of inorganic compounds in two principal ways: coordination polyhedra in which the vertices represent ligands surrounding a central atom which is often, but not always, a metal, and cluster polyhedra in which the vertices represent multivalent atoms and the edges represent bonding distances.

Among the polyhedra which arise in chemical contexts the regular icosahedron (Fig. 1) is of particular interest in terms of both its symmetry and topology. The symmetry point group [2] I_h, of the icosahedron, which has 120 operations, is the largest non-trivial point group; its rotation subgroup *I*, which has 60 operations, is isomorphic to the alternating group A_5 of even permutations of five objects. From the topological point of view the icosahedron is the largest deltahedron in which all vertices have degrees no higher than five. In this context a deltahedron is a polyhedron in which all of its faces are triangles and the degree of a vertex is the number of edges meeting at that vertex. Some deltahedra of chemical significance are depicted in Fig. 1.

A variety of inorganic substances have icosahedral structures; the following are of particular interest:

(1) the icosahedral boranes [3] $B_{12}H_{12}^{2-}$ and isoelectronic icosahedral carboranes [4] $C_2B_{10}H_{12}$ and their substitution products in which the external hydrogen atoms are replaced by other monovalent groups such as halogens and/or alkyl groups;

(2) elemental boron and metal borides having high boron content [5, 6];

(3) icosahedral quasicrystals based on aluminum icosahedra [7–10];

(4) icosahedral gallium ions Ga_{12}^{2-} found in intermetallic phases of gallium and alkali metals such as $RbGa_7[=Rb_2(Ga_{12})(Ga_2)]$ [11] and $K_3Ga_{13}[=K_6(Ga_{11})(Ga_{12})(Ga_3)]$ [12];

(5) icosahedral metal carbonyl clusters including both centered metal carbonyl clusters such as the rhodium carbonyl derivatives $[Rh_{12}Sb(CO)_{27}]^{3-}$ [13] and uncentered metal carbonyl clusters such as $[Ni_9(AsPh)_3(CO)_{15}]^{2-}$ and $[Ni_{10}(AsMe)_2(CO)_{18}]^{2-}$ containing Ni_9As_3 and $Ni_{10}As_2$ icosahedra, respectively [14];

0020-1693/92/$5.00

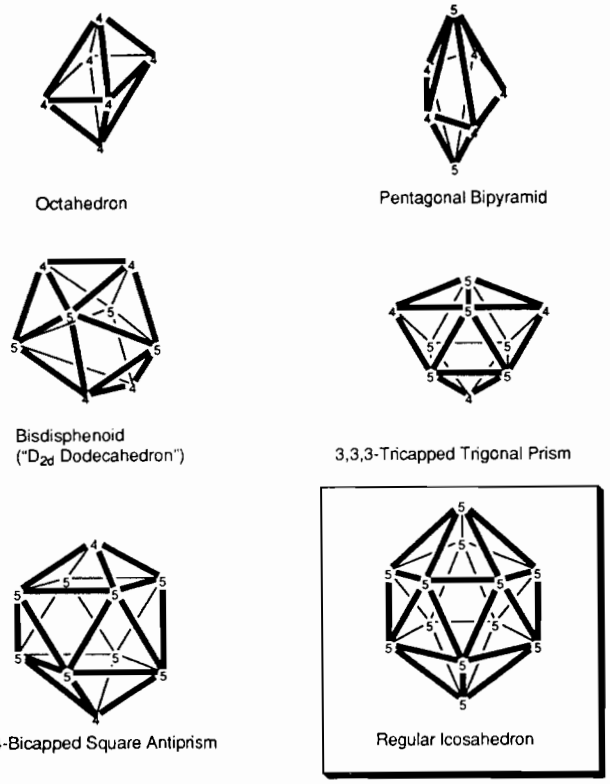

Fig. 1. The six deltahedra in which all vertices have degree 4 or 5. The vertices are labelled with their degrees (4 or 5).

(6) icosahedral gold clusters such as the centered icosahedron [15] $Au_{12}(Au)Cl_2(PMe_2Ph)_{10}^{3+}$ as well as much more complicated clusters based on icosahedral structural units [16] such as the 25-atom cluster $\{[(p\text{-}MeC_6H_4)_3P]_{10}Au_{13}Ag_{12}Br_8\}^+$ and the 38-atom cluster $[(p\text{-}MeC_6H_4)_3P]_{12}Au_{18}Ag_{20}Cl_{14}$;

(7) icosahedral polyoxometallates [17] such as the Silverton ions $M^{IV}Mo_{12}O_{42}^{8-}$ (M = Ce, Th, U) in which the central metal M^{IV} forms an MO_{12} icosahedron with the interior oxygen atoms.

The elements of the B, Al, Ga, ... column of the periodic table have a particularly high tendency to form structures based on E_{12} icosahedra (E = B, Al, Ga) as illustrated by examples (1)–(4) mentioned above; for this reason this column of the periodic table can be called the icosogens [18].

This paper presents a general survey of structure and bonding in icosahedral inorganic molecules with particular emphasis on topological aspects of delocalization and 'aromaticity' in such substances. First, however, aspects of the symmetry and topology of the icosahedron and other polyhedra of icosahedral symmetry will be reviewed.

2. Symmetry and topology of the icosahedron

The symmetry of the regular icosahedron (Fig. 1) relates to the special properties of its symmetry point group, namely I_h with 120 operations, as well as its subgroup of index 2 of pure rotations, namely I with 60 operations. Of particular interest are the relationships of these symmetry point groups to the symmetric group S_5 and the alternating group A_5 describing all $5! = 120$ permutations on five objects and all $5!/2 = 60$ even permutations on five objects, respectively. In order to understand these relationships some general ideas of group theory will first be reviewed [2].

Consider a group G. The number of operations in G, frequently designated as $|G|$, is called the order of G. Now let A and B be two operations of a group G with inverses A^{-1} and B^{-1}, respectively (i.e., $AA^{-1} = BB^{-1} = E$, the identity operation). If $AB = BA$ then A is said to commute with B. In addition $B^{-1}AB = C$ will be equal to some operation in G. The operation C is called the similarity transform of A by B and A and B may be said to be conjugate. A complete set of operations of a group G which are conjugate to one another is called a class (or more specifically a conjugacy class) of G. The number of operations in a conjugacy class is called its order; the orders of all conjugacy classes must be integral factors of the order of the group.

A group in which every operation commutes with every other operation is called a commutative group or an Abelian group after the famous Norwegian mathematician Abel (1802–1829) [19]. In an Abelian group every operation is in a conjugacy class by itself, i.e. all conjugacy classes are of order one. A normal subgroup N of G, written $N \lhd G$, is a subgroup of G which consists only of entire conjugacy classes of G [20]. A normal chain of a group G is a sequence of normal subgroups $C_1 \lhd N_{a_1} \lhd N_{a_2} \lhd N_{a_3} \lhd \ldots \lhd N_{a_s} \lhd G$, in which s is the number of normal subgroups (besides C_1 and G) in the normal chain. If such a chain starts with the identity group C_1 and leads to G and if all of the quotient groups $N_{a_1}/C_1 = C_{a_1}$, $N_{a_2}/N_{a_1} = C_{a_2}$, ..., $G/N_{a_s} = C_{a_{s+2}}$ are cyclic, then G is a composite or soluble group. Otherwise G is a simple group. Simple groups are particularly important in the theory of finite groups [21]. The icosahedral pure rotational group I is of significance in group theory in being the smallest non-trivial simple group.

Now let us consider the properties of the permutation groups on small numbers of objects. In this context the symmetric group S_n is a group consisting of all possible $n!$ permutations of n objects whereas the alternating group A_n is a group consisting of all possible $n!/2$ even permutations of n objects. The alternating group A_3 and the symmetric group S_3 on three objects are isomorphic with the point groups C_3 and D_3, respectively. The latter two point groups correspond to the symmetry of the two-dimensional simplex [22], i.e. to a planar triangle. Similarly, the alternating group

A_4 and symmetric group S_4 on four objects are, respectively, isomorphic with the point groups T and T_d, which correspond to the symmetry of the three-dimensional simplex, i.e. to that of the regular tetrahedron. The alternating group on five objects, A_5, has $5!/2=60$ operations like the icosahedral pure rotation group I. Similarly, both the symmetric group S_5 and the full icosahedral point group, I_h, have $5!=120$ operations. Examination of the conjugacy class structure [19, 23] of the permutation groups A_5 and S_5 on the one hand and that of the icosahedral point groups I and I_h, on the other hand, reveals that they correspond to each other by the relationships

$$I \cong A_5 \text{ (isomorphism)} \tag{1}$$

$$S_5 = A_5 \wedge S_2 \text{ (semi-direct product)} \tag{2}$$

$$I_h = I \times C_2 \text{ (direct product)} \tag{3}$$

In this context a group G is a direct product of two groups A and B (i.e., $G=A\times B$) when:

(i) for any $a\in A$ and any $b\in B$ the automorphism $\phi(b)$ of A is the identity thus

$$\phi(b)a = a \tag{4}$$

(ii) there is an isomorphism between G and the group of pairs (a,b) with $a\in A$ and $b\in B$ which satisfies the multiplication law

$$(a_1,b_1)(a_2,b_2) = (a_1a_2, b_1b_2) \tag{5}$$

Similarly a group G is a semi-direct product of two groups A and B (i.e., $G=A\wedge B$) when:

(i) for any $a\in A$ and any $b\in B$ there is an automorphism $\phi(b)$ of A such that:

$$\phi(b_1)[\phi(b_2)a] = \phi(b_1b_2)a \tag{6}$$

(ii) there is an isomorphism between G and the group of pairs (a,b) with $a\in A$ and $b\in B$ which satisfies the multiplication law

$$(a_1,b_1)(a_2,b_2) = (a_1[\phi(b_1)a_2], b_1b_2) \tag{7}$$

A direct product is thus a special case of a semi-direct product.

Let us now consider the S_n permutation groups having $n!$ operations. In these groups permutations having different cycle structures necessarily belong to different conjugacy classes. Moreover, for these specific groups a common partition will be a guarantee that the elements do in fact belong to the same class. Thus, the conjugacy classes of the permutation groups A_5 and S_5 are indicated in terms of their cycle indices [24, 25] Z(G) in the following way

$$60Z(A_5) = x_1^5 + 20x_1^2x_3 + 15x_1x_2^2 + 24x_5 \tag{8}$$

$$120Z(S_5) = x_1^5 + 10x_1^3x_2 + 20x_1^2x_3 + 15x_1x_2^2 + 30x_1x_4 + 20x_2x_3 + 24x_5 \tag{9}$$

Furthermore the conjugacy classes of the icosahedral point groups I and I_h are indicated from their character tables to be the following (using S_{10} and S_6 to represent improper rotations rather than symmetric groups)

$$I = \{E,\ 12C_5,\ 12C_5^2,\ 20C_3,\ 15C_2\} \tag{10}$$

$$I_h = \{E,\ 2C_5,\ 12C_5^2,\ 20C_3,\ 15C_2,\ i,\ 12S_{10}^3,\ 12S_{10},\ 20S_6,\ 15\sigma\} \tag{11}$$

Comparison of eqns. (8) and (9) with eqns. (10) and (11), respectively, by using the relationships in eqns. (1), (2) and (3) leads to the following observations:

(i) The class of A_5 represented by the cycle index turn $24x_5$ corresponds to the two classes $12C_5$ and $12C_5^2$ of I taken together.

(ii) In the point group I_h, each class of improper rotations (i, S_{10}, S_{10}^3, S_6, and σ) corresponds to a class of proper rotations of the same size, namely to E, C_5, C_5^2, C_3, and C_2, respectively, whereas the classes of S_5 are not partitioned analogously.

The relationship between the icosahedral point groups I_h and I outlined here and the permutation groups A_5 and S_5 is discussed in more detail elsewhere [26].

Now let us consider some aspects of the topology of the icosahedron. The icosahedron is an example of a deltahedron in which all vertices have degrees 4 or 5; in this context a deltahedron is a polyhedron in which all faces are triangles and the degree of a vertex is the number of edges meeting at that vertex. There are only six topologically possible deltahedra in which all vertices have degrees 4 or 5; these special deltahedra are depicted in Fig. 1. The octahedron in which all vertices have degree 4 and the icosahedron in which all vertices have degree 5 are the end members of this series. Note that there is exactly one deltahedron for each number of vertices from 6 to 12 with the exception of 11; the deltahedra depicted in Fig. 1 are actually found in the boranes $B_nH_n^{2-}$ ($n=6$, 7, 8, 9, 10 and 12) [27]. A deltahedron with 11 vertices all of degrees 4 or 5 has been shown to be topologically impossible [28]; the deltahedron actually found for the borane $B_{11}H_{11}^{2-}$ has one vertex of degree 6 [29].

The next question of interest is the topological relationship of the icosahedron to other polyhedra having 12 vertices. As early as 1966 Lipscomb [30] described framework rearrangements (isomerizations) in boranes and carboranes in terms of diamond-square-diamond (dsd) processes. Such a dsd process in a polyhedron occurs at two triangular faces sharing an edge and can be depicted as follows where a dsd process corresponds to **Ia → Ib → Ic:**

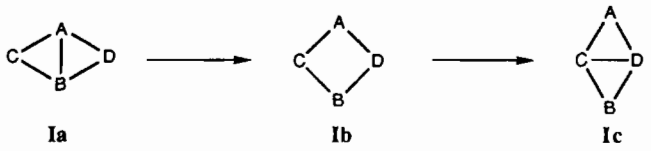

The first stage of a dsd process, i.e. **Ia → Ib**, may be called a diamond-square process. Of particular interest is the conversion of an icosahedron to a cuboctahedron (Fig. 2) by means of a sextuple diamond-square process, i.e. six diamond-square processes in parallel so configured to lead to O_h symmetry in the final cuboctahedron; this process was described in ref. 30. Such a conversion from an icosahedron to a cuboctahedron will have a tendency to occur either to increase the cavity of the 12-vertex polyhedron in order to accommodate a larger interstitial atom or to change the local symmetry from I_h to O_h in order to improve the packing in an infinite three-dimensional lattice. The result of a single diamond-square process is to reduce the numbers of both the edges and faces by one as indicated by the conversion **Ia → Ib** depicted above. Thus a sextuple diamond-square process converts an icosahedron with 30 edges and 20 faces to a cuboctahedron with 24 (i.e 30 − 6) edges and 14 (i.e. 20 − 6) faces. Of the 14 faces of the cuboctahedron, six are the squares generated by the diamond-square process and the remaining eight are triangular faces of the original icosahedron.

In generating polyhedra, including those of icosahedral symmetry, the operations of capping and dualization are important. Capping a polyhedron P_1 consists of adding a new vertex above the center of one of its faces F_1 followed by adding edges to connect the new vertex with each vertex of F_1. This capping process gives a new polyhedron P_2 having one more vertex than P_1. If a triangular face is capped, the following relationships will be satisfied where the subscripts 1 and 2 refer to P_1 and P_2, respectively: $v_2 = v_1 + 1$; $e_2 = e_1 + 3$; $f_2 = f_1 + 2$. A given polyhedron P can be converted into its dual P* by locating the centers of the faces of P* at the vertices of P and the vertices of P* above the centers of the faces of P. Two vertices in the dual P* are connected by an edge when the corresponding faces in P share an edge. The process of dualization has the following properties:

Fig. 2. The sextuple diamond-square process for conversion of the icosahedron to the cuboctahedron.

(i) the numbers of vertices and edges in a pair of dual polyhedra P and P* satisfy the relationship $v^* = f$, $e^* = e$, $f^* = v$;

(ii) dual polyhedra have the same symmetry elements and thus belong to the same symmetry point group; thus a dual of a polyhedron with icosahedral (I_h) symmetry also has I_h symmetry;

(iii) dualization of the dual of a polyhedron leads to the original polyhedron;

(iv) the degrees of the vertices of a polyhedron correspond to the number of edges in the corresponding face polygons of its dual.

Figure 3 shows three pairs of dual polyhedra having I_h symmetry. The dual of the icosahedron is the regular dodecahedron. The dual of the truncated icosahedron (the 'C_{60} polyhedron') is the omnicapped dodecahedron, which can be generated by capping each of the 12 pentagonal faces of the regular dodecahedron. The dual of the icosidodecahedron with 30 vertices of degree 4, 60 edges and 32 faces is the rhombic triacontahedron with 32 vertices, 60 edges and 30 identical diamond faces.

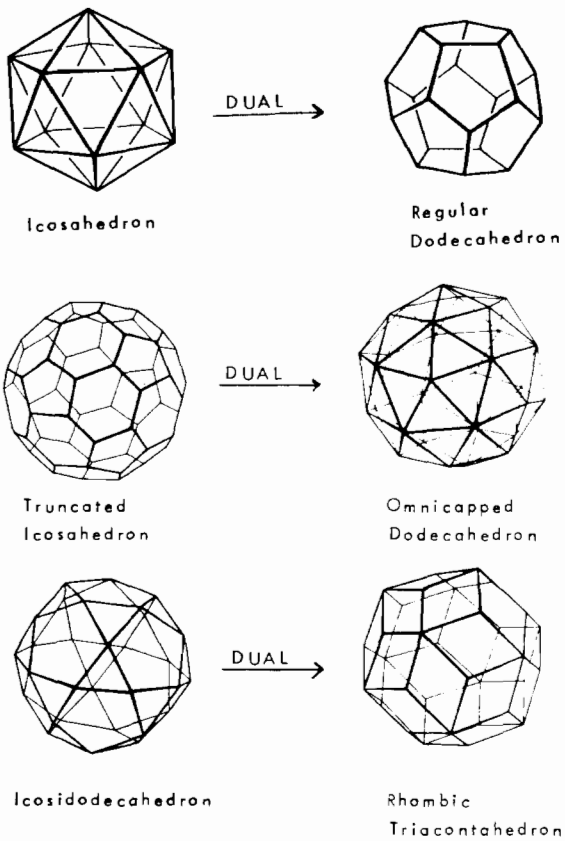

Fig. 3. Three pairs of dual polyhedra having icosahedral (I_h) point group symmetry.

3. Icosahedral clusters: globally delocalized molecules and ions

This section discusses the properties of globally delocalized icosahedral clusters. The prototypical icosahedral clusters are the deltahedral boranes $B_{12}H_{12}^{2-}$ and the isoelectronic carboranes $C_2B_{10}H_{12}$. The chemical bonding topologies of these icosahedral clusters are the simplest to understand since the vertex boron and/or carbon atoms use sp^3 manifolds having only four valence orbitals with no involvement of d orbitals in chemical bonding. The graph-theory derived method for studying the chemical bonding topology of icosahedral clusters is first illustrated by $B_{12}H_{12}^{2-}$. Subsequent discussion focusses on intermetallic phases of alkali metals and gallium, which is a heavier congener of boron. In addition, globally delocalized metal icosahedra in nickel carbonyl and rhodium carbonyl clusters are also discussed.

The topology of a chemical bonding network can be represented by a graph, G, in which the vertices correspond to atoms or orbitals participating in the chemical bonding and the edges correspond to bonding relationships. The adjacency matrix [31] **A** of such a graph can be defined as follows:

$$A_{ij}=\begin{cases}0 \text{ if } i=j\\ 1 \text{ if } i \text{ and } j \text{ are connected by an edge}\\ 0 \text{ if } i \text{ if } i \text{ and } j \text{ are not connected by an edge}\end{cases} \tag{12}$$

The eigenvalues of the adjacency matrix are obtained from the following determinantal equation:

$$|\mathbf{A}-x\mathbf{I}|=0 \tag{13}$$

in which **I** is the unit matrix ($I_{ii}=1$ and $I_{ij}=0$ for $i\neq j$). The polynomial derived from eqn. 13 is known as the characteristic polynomial of the graph G. These topologically derived eigenvalues are closely related to the energy levels as determined by Hückel theory which uses the secular equation

$$|\mathbf{H}-E\mathbf{S}|=0 \tag{14}$$

Note the general similarities between eqns. (13) and (14). In eqn. 14 the energy matrix **H** and the overlap matrix **S** can be resolved into the identity matrix **I** and the adjacency matrix **A** as follows:

$$\begin{aligned}\mathbf{H}&=\alpha\mathbf{I}+\beta\mathbf{A}\\ \mathbf{S}&=\mathbf{I}+S\mathbf{A}\end{aligned} \tag{15}$$

The energy levels of the Hückel molecular orbitals (eqn. (14)) are thus related to the eigenvalues x_k of the adjacency matrix **A** (eqn. (13)) by eqn. (16) [32–35].

$$E_k=\frac{\alpha+x_k\beta}{1+x_kS} \tag{16}$$

In eqn. (16) α is the standard Coulomb integral, assumed to be the same for all atoms, β is the resonance integral, taken to be the same for all bonds, and S is the overlap integral between atomic orbitals on neighboring atoms. Positive and negative eigenvalues x_k from eqn. (16) thus correspond to bonding and antibonding orbitals, respectively. Figure 4 illustrates the spectra of the icosahedron and the closely related cuboctahedron obtained from their adjacency matrices using the symmetry factoring procedures [36] depicted in Fig. 5 for the icosahedron and Fig. 6 for the cuboctahedron. Note that because of the high symmetry most of the eigenvalues are degenerate; i.e. the same eigenvalue appears as a repeated root. Thus for the regular icosahedron the eigenvalue -1 appears five times, the two eigenvalues $\pm\sqrt{5}$ each appear three times, and only the most positive eigenvalue $+5$ appears only once.

A difficulty in applying eqn. 16 is the need to determine three parameters α, β and S to relate the eigenvalues x_k to the corresponding molecular orbital energies E_k. Any actual system, even highly symmetrical icosahedral systems, provides too few relationships to determine fully all of these three parameters. Therefore some assumptions concerning the values of α, β and S are necessary in order to make the use of eqn. 16 tractable. The approach that is generally taken is to assume a zero value for S thereby reducing eqn. (16) to the linear equation

$$E_k=\alpha+x_k\beta \tag{17}$$

The value of α can then be determined from the midpoint of all of the molecular orbital energy parameters through taking an appropriately weighted average. The third parameter, β, is obtained from specific orbital energies.

The two extreme types of skeletal chemical bonding formed by polyhedral clusters of atoms such as polyhedral boranes or metal clusters may be called edge-localized and globally delocalized [37]. An edge-localized polyhedron has two-electron, two-center bonds along each edge of the polyhedron and is favored when

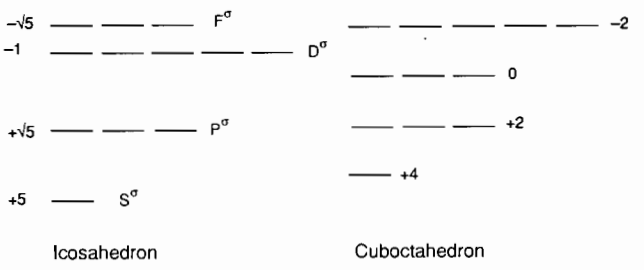

Fig. 4. The spectra of the icosahedron and the cuboctahedron. The eigenvalues for the icosahedron are given the designations S^σ, P^σ, D^σ and F^σ of tensor surface harmonic theory.

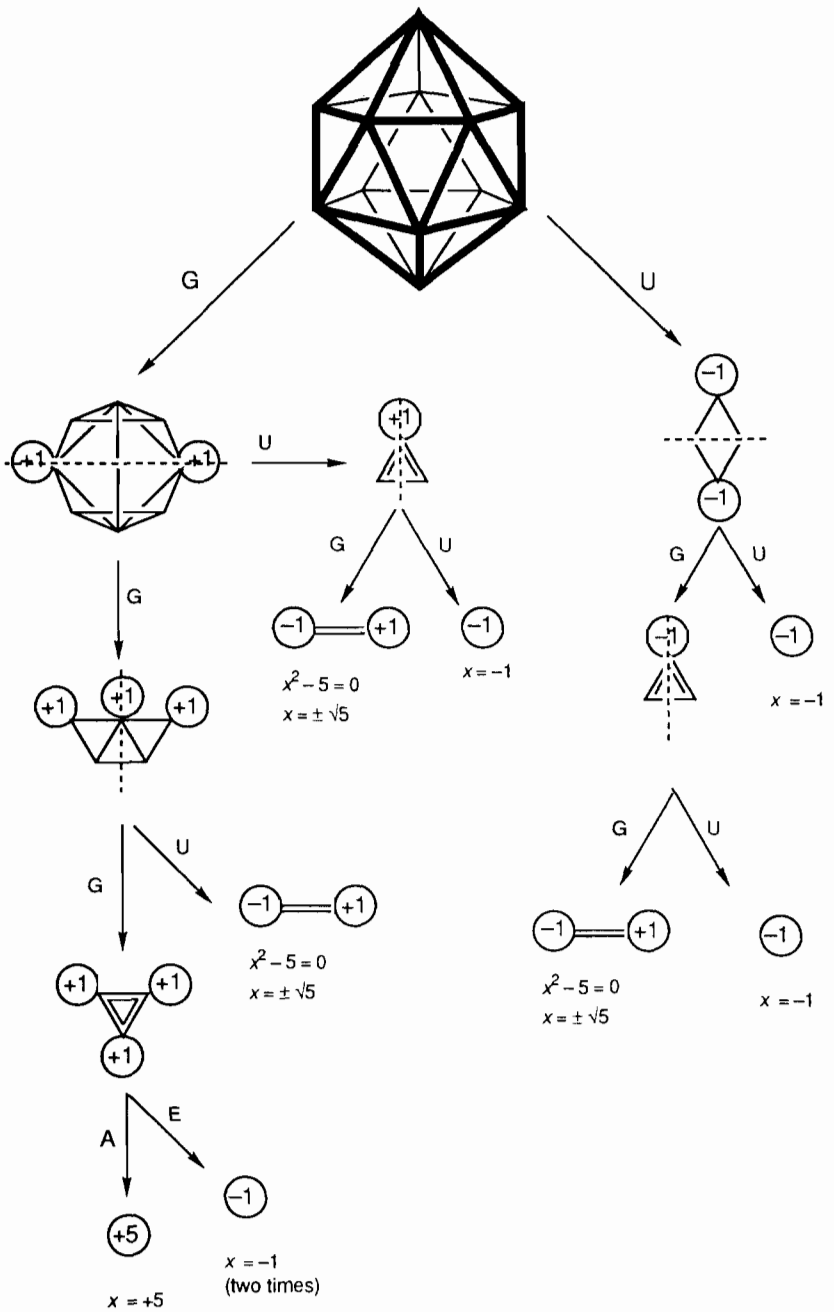

Fig. 5. Symmetry factoring of the icosahedron to determine its eigenvalues using the procedure outlined in ref. 36.

the numbers of internal orbitals from the vertex atoms match the vertex degrees. A globally delocalized polyhedron has a multicenter bond in the center of the polyhedron and is favored when the numbers of internal orbitals of the vertex atoms do not match the vertex degrees. Fully globally delocalized polyhedra are deltahedra having no vertices of degree 3 (Fig. 1) including the icosahedron. In the case of the 'light' vertex atoms carbon and boron having only the four orbitals of the sp^3 manifold, only three orbitals can be internal orbitals. Since all vertices of an icosahedron have degree 5, icosahedra of boron and other light atoms (e.g. carbon and nitrogen) must necessarily be globally delocalized since the degree 5 vertices of the icosahedron do not match the three internal orbitals of the vertex atoms.

Let us now consider some important features of the chemical bonding topology in the icosahedral borane anion $B_{12}H_{12}^{2-}$. The vertex B–H unit in a deltahedral borane anion such as $B_{12}H_{12}^{2-}$ can be depicted as follows:

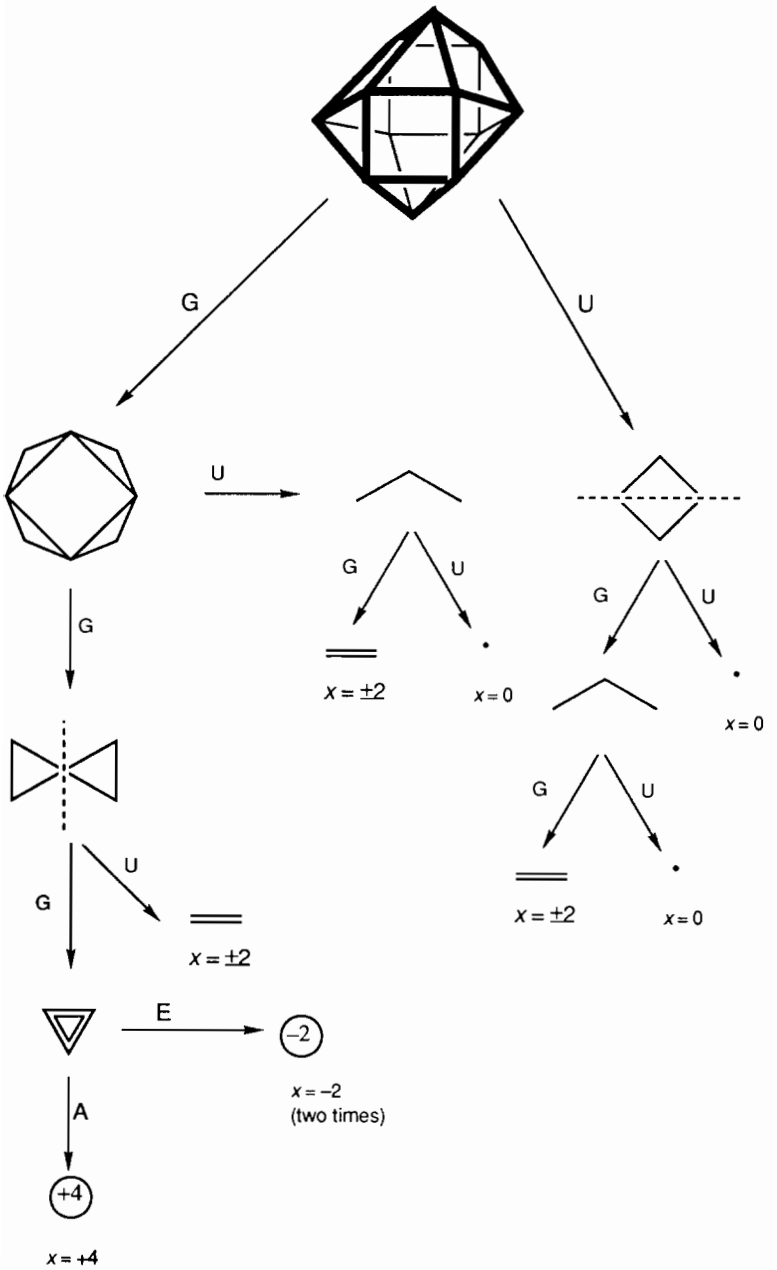

Fig. 6. Symmetry factoring of the cuboctahedron to determine its eigenvalues using the procedure outlined in ref. 36.

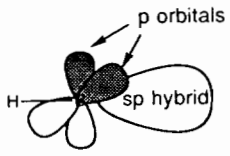

II

In this structure the boron atom has two anodal sp hybrids, one of which participates in the skeletal bonding; this sp hybrid orbital is called a unique internal orbital or a radial [38, 39] orbital. Since the unique internal orbital is anodal (i.e. has no nodes), the deltahedral boranes can be regarded as anodal aromatic systems. In addition the two p orbitals on the boron vertex depicted in **II** participate in the skeletal bonding as twin internal orbitals or tangential orbitals. Pairwise overlap between the (2)(12) = 24 twin internal orbitals is responsible for chemical bonding in the surface of the icosahedron and leads to the splitting of these 24 orbitals into 12 bonding and 12 antibonding orbitals. The magnitude of this splitting may be designated as $2\beta_s$, where β_s relates to the parameter β in eqns. (12) and (13).

The surface bonding in $B_{12}H_{12}^{2-}$ is supplemented by additional bonding and antibonding orbitals formed

by global mutual overlap of the 12 unique internal orbitals, namely the sp hybrids oriented away from the B–H bond depicted in **II**. This portion of the chemical bonding topology results in a 12-center bond directed towards the center of the icosahedron. This core bonding can be represented by a graph G_c in which the vertices correspond to the vertex atoms of the deltahedron or equivalently their unique internal orbitals and the edges represent pairs of overlapping unique internal orbitals. The relative energies E_c of the additional molecular orbitals arising from the core bonding are determined from the eigenvalues x_c of the adjacency matrix $\mathbf{A}_c$ of the graph of the icosahedron using β or more specifically β_c as the energy unit (eqns. (16) and (17)). The ratio β_c/β_s measures the magnitude of the core interactions involving the unique internal orbitals relative to the surface interactions between the twin internal orbitals.

A critical question is the nature of the core bonding graph G_c for the icosahedral borane $B_{12}H_{12}^{2-}$. The two limiting possibilities for G_c are the complete graph K_{12} and the deltahedral graph D_{12} and the corresponding core bonding topologies can be called the complete and deltahedral topologies, respectively. In the complete graph K_{12} each of the twelve vertices has an edge going to every other vertex leading to a total of (12)(11)/2=66 edges [40]. The spectrum of the complete graph K_{12} has only one positive eigenvalue, namely +11; the remaining 11 eigenvalues are all negative, namely −1. The deltahedral graph D_{12} corresponds to the 1-skeleton of the icosahedron thus having 12 vertices and 30 edges. The D_{12} graph has the four positive eigenvalues, namely +5 and $+\sqrt{5}$ three times. The +5 eigenvalue, like the most positive eigenvalues of other deltahedra, may be called the principal eigenvalue of the icosahedron. Note that in Fig. 5 the principal eigenvalue arises from the fully symmetric pathway of the symmetry factoring scheme used to determine the spectrum of the icosahedron, namely the pathway using G components at branches from two-fold symmetry operations and the A component at the final branch from the three-fold symmetry operation. The highly bonding molecular orbital corresponding to the principal eigenvalue of G_c may be called the principal core orbital.

The icosahedral borane $B_{12}H_{12}^{2-}$ has 26 skeletal electrons calculated as follows:

12 B–H vertices contributing 2 skeletal electrons each: (12)(2)=	24 electrons
−2 charge:	2 electrons
Total skeletal electrons:	26 electrons

Note that the surface bonding uses 24 of these electrons leaving only two electrons for the core bonding corresponding to a single core bonding molecular orbital and a single positive eigenvalue for G_c. Thus only if G_c is taken to be the corresponding complete graph K_{12} will this simple model given above for a globally delocalized icosahedron give the correct 26 skeletal electrons. Such a model with complete core bonding topology is the basis for the graph-theory derived model for the chemical bonding topology of deltahedral boranes and metal clusters discussed in previous papers [27, 28, 41, 42]. However, deltahedral core bonding topology, based on the D_{12} graph of the icosahedron, can also account for the observed 26 skeletal electrons in the case of $B_{12}H_{12}^{2-}$ if there is a mechanism of raising the energies of all of the core molecular orbitals, other than the principal core orbital, to antibonding energy levels. The original graph–theoretical analysis [43] of the 3*n* Hoffmann–Lipscomb LCAO-MO extended Hückel computations [44] on icosahedral $B_{12}H_{12}^{2-}$ showed that four core orbitals would be bonding orbitals except for core-surface orbital mixing which raises the energies of three of these four core orbitals to antibonding levels leaving only the principal core orbital as a bonding core orbital.

These ideas concerning the skeletal bonding in $B_{12}H_{12}^{2-}$ and other deltahedral borane anions can be related to tensor surface harmonic theory as developed by Stone *et al.* [45, 46] and elaborated by Johnston and Mingos [47]. The orbitals of the Γ_σ representation such as the 12 core orbitals in $B_{12}H_{12}^{2-}$ correspond to the (scalar) spherical harmonics which for the B_{12} icosahedron correspond successively to the single S^σ, the three P^σ, the five D^σ, and three of the seven F^σ orbitals of increasing energy and nodality. These labels are shown in Fig. 4 for the corresponding eigenvalues of the icosahedron. The orbitals of the Γ_π representation such as the surface orbitals correspond to the vector spherical harmonics which for the icosahedron correspond successively to three P^π, five D^π, and four of the F^π antibonding/bonding orbital pairs of increasing energy and nodality. This relates to the following aspects of the graph theory derived model for the skeletal bonding in deltahedral boranes.

(i) The principal core orbital corresponds to the S^σ orbital in tensor surface harmonic theory. Since there are no S^π or $\bar{S}^\pi$ surface orbitals, the principal (S^σ) core orbital in $B_{12}H_{12}^{2-}$, corresponding to the +5 eigenvalue of the icosahedron (Figs. 4 and 5) cannot mix with any surface orbitals in accord with ideas discussed above.

(ii) The three core orbitals of lowest energy other than the principal (S^σ) core orbital are the P^σ orbitals in tensor surface harmonic theory. These orbitals correspond to the three most positive eigenvalues other than the principal eigenvalue of the corresponding deltahedron, namely the three $+\sqrt{5}$ eigenvalues of the icosahedron in the case of $B_{12}H_{12}^{2-}$. The P^σ core orbitals mix with the P^π surface orbitals so that the P^σ core orbitals become antibonding with concurrent lowering

of the energies of the P^{π} surface orbitals below the energies of the other surface bonding orbitals. Thus in computations of orbital energies of deltahedral borane anions, the lowest lying molecular orbital is the principal (S^{σ}) core orbital and the next lowest lying orbitals are three P^{π} surface orbitals which are degenerate in the case of $B_{12}H_{12}^{2-}$. This ordering of the lowest lying molecular orbitals is particularly apparent in the MNDO computations presented by Brint *et al.* [48]. However, their label of P^{σ} rather than P^{π} for the three orbitals immediately above the principal core orbital S^{σ} obscures the relationship of their computed molecular orbitals to those predicted by the graph-theory derived method.

The icosahedral borane anion $B_{12}H_{12}^{2-}$ and the isoelectronic carborane $C_2B_{10}H_{12}$ are the prototypical examples of simple molecules based on globally delocalized icosahedra. However, other more electropositive elements can form icosahedral clusters in which the same principles of globally delocalized bonding can apply.

Consider first a congener of boron, namely gallium. Gallium forms a number of intermetallic phases with alkali metals based on globally delocalized gallium deltahedra [49], such species can be conveniently called alkali metal gallides. The gallium vertices in the deltahedra in alkali metal gallides may be regarded as having an sp^3d^5 manifold of nine valence orbitals, but with all five of the d orbitals having non-bonding electron pairs. Thus only the four orbitals from the sp^3 manifold participate in the metal cluster bonding as is the case for boron vertices. Among these four valence orbitals, three are normally used for intrapolyhedral skeletal bonding, leaving the fourth orbital for bonding to an external group, usually a two-center bond to a gallium vertex of an adjacent deltahedron or to an extra 'satellite' gallium atom between the gallium deltahedra. A gallium vertex contributing one electron to a two-center external bond functions as a donor of two skeletal electrons like the BH vertices in the $B_nH_n^{2-}$ deltahedra.

The structures of the alkali metal gallides consist of infinite networks of gallium polyhedra with alkali metals in some of the interstices. The alkali metals can be assumed to form monopositive ions thereby donating one electron to the gallium network for each alkali metal atom.

The simplest examples of alkali metal gallides containing Ga_{12} icosahedra are the derivatives of stoichiometries MGa_7 (M=Rb, Cs) [11] which may be represented more precisely as $M_2(Ga_{12})(Ga_2)$. These structures have not only a Ga_{12} icosahedron but also a bonded pair (Ga–Ga=2.52 Å) of four-coordinate satellite gallium atoms (Ga(4) in ref. 11). Six of the gallium vertices of each Ga_{12} icosahedron are bonded externally to other gallium atoms through two-center two-electron bonds whereas the other six gallium vertices are bonded externally to other gallium atoms through three-center two-electron bonds. In such a situation the 26 skeletal electron closed-shell electronic configuration of a gallium icosahedron is not the usual Ga_{12}^{2-} ion but neutral Ga_{12} determined as follows:

Valence electrons of 12 Ga atoms: (12)(3)=	36 electrons
Required for 6/2 external 2-center 2-electron bonds: (6/2)(2)=	−6 electrons
Required for 6/3 external 3-center 2-electron bonds: (6/3)(2)=	−4 electrons
Net electrons remaining for skeletal electrons:	26 electrons

The closed shell electronic configurations of Ga_{12} for the gallium icosahedra and Ga_2^{2-} for the bonded pairs of four-coordinate satellite atoms leads to the observed stoichiometry $M_2(Ga_{12})(Ga_2)=MGa_7$.

A more complicated alkali metal gallide is the phase K_3Ga_{13}, which may be represented as $K_6(Ga_{11})(Ga_{12})(Ga)_3$ with equal numbers of Ga_{11} and Ga_{12} deltahedra and three satellite gallium atoms for each 23 (i.e. $Ga_{11}+Ga_{12}$) deltahedral gallium atoms [12]. Each vertex atom in both types of gallium deltahedra forms one two-center two-electron external bond leading to the closed shell electron configurations Ga_{11}^{2-} and Ga_{12}^{2-} similar to the corresponding deltahedral boranes $B_nH_n^{2-}$ ($n=11$, 12). There are both three-coordinate (Ga(4) in ref. 12) and four-coordinate (Ga(11) in ref. 12) satellite gallium atoms with twice as many four-coordinate as three-coordinate satellite gallium atoms. The electronic configurations of Ga_{11}^{2-} and Ga_{12}^{2-} for the gallium deltahedra, Ga^- for the four-coordinate satellite gallium atoms and Ga for the three-coordinate satellite gallium atoms leads to the observed stoichiometry $K_6(Ga_{11})(Ga_{12})(Ga^{3\text{-coord}})(Ga^{4\text{-coord}})_2=K_6Ga_{26}=K_3Ga_{13}$.

Metal icosahedra are also found in transition metal carbonyl clusters. In such clusters the transition metal vertices normally have nine-orbital sp^3d^5 manifolds with the normal three internal orbitals leaving six orbitals per vertex for the external bonding. Nickel carbonyl derivatives are a prolific source of such structures. Thus reactions of $Ni_6(CO)_{12}^{2-}$ with halides of germanium, tin, arsenic and antimony lead to nickel carbonyl clusters having five-fold symmetry based on the icosahedron (Fig. 7). Such clusters include the uncentered icosahedra $Ni_9(AsPh)_3(CO)_{15}^{2-}$ and $Ni_{10}(AsMe)_2(CO)_{18}^{2-}$ [13], the centered icosahedra $Ni_{12}E(CO)_{22}^{2-}$ (E=Ge, Sn) [50], the pentagonal antiprism $Ni_{10}Ge(CO)_{20}^{2-}$ derived from an icosahedron by removal of two antipodal vertices [50] and the nickel-centered icosahedron $Ni_{13}Sb_2(CO)_{24}^{4-}=Ni_{10}[SbNi(CO)_3]_2(Ni)(CO)_{18}^{4-}$ [51]. In addition, rhodium forms the icosahedral cluster anion $Rh_{12}Sb(CO)_{27}^{3-}$ [13], which has an antimony atom in the center (Fig. 7). All of these icosahedral metal carbonyl clusters have the 26 skeletal electrons cor-

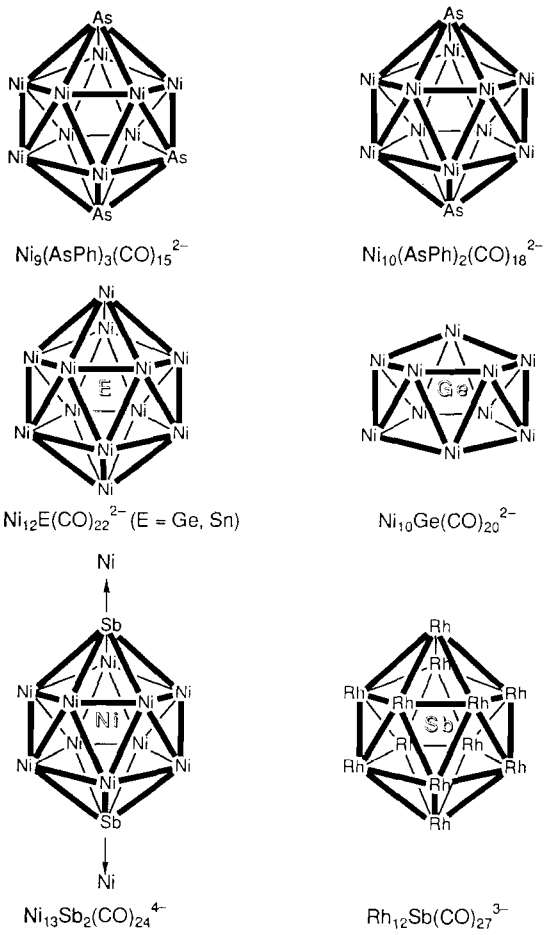

Fig. 7. The metal frameworks of six icosahedral metal carbonyl clusters. The interstitial atoms are shown in the four clusters containing interstitial atoms.

responding to a globally delocalized icosahedron. The skeletal electron counts for these clusters are obtained as follows:

(1) $Ni_9(AsPh)_3(CO)_{15}^{2-}$: $18-6+12+2=26$ skeletal electrons arising from 9 $Ni(CO)_2$ vertices, a deficit of 3 CO groups, the 3 AsPh vertices, and the -2 charge, respectively;

(2) $Ni_{10}(AsMe)_2(CO)_{18}^{2-}$: $20-4+8+2=26$ skeletal electrons arising from 10 $Ni(CO)_2$ vertices, a deficit of 2 CO groups, the 2 AsMe vertices, and the -2 charge, respectively;

(3) $Ni_{12}E(CO)_{22}^{2-}$ (E = Ge, Sn): $24-4+4+2=26$ skeletal electrons arising from 12 $Ni(CO)_2$ vertices, a deficit of 2 CO groups, the interstitial Ge or Sn atom, and the -2 charge, respectively;

(4) $Ni_{10}Ge(CO)_{20}^{2-}$: $20+4+2=26$ skeletal electrons arising from 10 $Ni(CO)_2$ vertices, the interstitial Ge atom, and the -2 charge, respectively;

(5) $Ni_{13}Sb_2(CO)_{24}^{4-} = Ni_{10}[SbNi(CO)_3]_2(Ni)(CO)_{18}^{4-}$: $20-4+6+0+4=26$ skeletal electrons arising from 10 $Ni(CO)_2$ vertices, a deficit of 2 CO groups, the 2 $SbNi(CO)_3$ vertices, the interstitial Ni atom, and the -4 charge;

(6) $Rh_{12}Sb(CO)_{27}^{3-}$: $12+6+5+3=26$ skeletal electrons arising form 12 $Rh(CO)_2$ vertices, a surplus of 3 CO groups, the interstitial Sb atom, and the -3 charge, respectively.

These electron counting schemes consider the following points.

(i) The electron counting is independent of whether the metal carbonyl groups are terminal or bridging. Thus either terminal or bridging carbonyl groups are two-electron donors.

(ii) An $Ni(CO)_2$ vertex is a donor of 10 (Ni^0) + 4 (2 CO) − 12 (6 external orbitals) = 2 skeletal electrons and a $Rh(CO)_2$ vertex is a donor of 9 (Rh^0) + 4 (2 CO) − 12 (6 external orbitals) = 1 skeletal electron.

(iii) Interstitial germanium and tin atoms are donors of four skeletal electrons each and an interstitial antimony atom is a donor of five skeletal electrons since such interstitial atoms have no external orbitals. The interstitial nickel atom in $Ni_{13}Sb_2(CO)_{24}^{4-}$, which is surrounded by an icosahedron of nickel atoms, is a donor of zero skeletal electrons since its ten valence electrons are d electrons which must go into the H_g antibonding level of the Ni_{12} icosahedron corresponding to the -1 eigenvalue (Fig. 4). These nickel d electrons thus cannot participate in skeletal bonding. Furthermore, the reported oxidation of $Ni_{13}Sb_2(CO)_{24}^{4-}$ to $Ni_{13}Sb_2(CO)_{24}^{3-}$ and $Ni_{13}Sb_2(CO)_{24}^{2-}$ can simply involve removal of one or two of the essentially nonbonding nickel d electrons which should affect very little the total energy of the cluster.

The icosahedral clusters $Ni_{12}E(CO)_{22}^{2-}$ (E = Ge, Sn), $Ni_{13}Sb_2(CO)_{24}^{4-}$ and $Rh_{12}Sb(CO)_{27}^{3-}$ have structures with an interstitial atom in the center of an Ni_{12} or Rh_{12} icosahedron. In some cases the volume requirements of an interstitial atom can lead to expansion of an icosahedral cavity to a cuboctahedral cavity by means of the sextuple diamond-square process depicted in Fig. 2, since the volume of a polyhedron containing an interstitial atom can be increased by decreasing the number of edges. The positive eigenvalues of the spectrum of a cuboctahedron are very similar to those of the icosahedron (Fig. 4). Therefore an cuboctahedron can function as a globally delocalized (2)(12) + 2 = 26 skeletal electron 12-vertex polyhedron just like the icosahedron. An excellent example of a globally delocalized centered cuboctahedral metal carbonyl cluster is the rhodium carbonyl anion [52] $Rh_{12}(Rh)(CO)_{24}H_3^{2-}$ which has the required 26 skeletal electrons from the following electron counting scheme:

12 $Rh(CO)_2$ vertices: (12)[9−(4)(2)] =	12 electrons
Interstitial rhodium atom	9 electrons
3 hydrogen atoms: (3)(1) =	3 electrons
−2 charge:	2 electrons
Total skeletal electrons	26 electrons

The coinage metals silver and gold also form some icosahedral clusters for which the globally delocalized bonding schemes outlined above appear to be applicable with some modification. A specific feature of the chemistry of gold (and to a lesser extent silver) is the shifting of one or two of the outer p orbitals to such high energies that they no longer participate in the chemical bonding [53]. If two of the outer p orbitals of a gold vertex are so shifted, then there remains only one p orbital in the valence orbital manifold, which now contains 7 orbitals (spd^5) and has cylindrical symmetry extending in one axial dimension much further than the other two dimensions. Filling this spd^5 manifold with electrons leads to the 14-electron configuration found in two-coordinate linear complexes of the d^{10} metals such as Pt(0), Au(I), Au(I), Hg(II) and Tl(III). The raising of one or particularly two outer p orbitals to antibonding levels has been attributed to relativistic effects [54].

Thus to an initial approximation the spd^5 orbital manifold of an L→Au or X−Au vertex (L = tertiary phosphine or isocyanide ligand; X = halogen or pseudohalogen) in a polyhedral gold cluster may be regarded as having a pair of linear sp hybrids depicted schematically as follows:

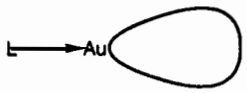

III

One of these hybrids, corresponding to the unique internal orbital discussed above, points towards the center of the polyhedron and thus can participate in the core bonding discussed above. The other sp hybrid corresponds to the external orbital in the above bonding model and overlaps with the bonding orbital from the L (as in **III**) or X ligand. In this initial approximation, the five d orbitals of the gold vertex are essentially non-bonding and are filled with electron pairs thereby using 10 of the 11 valence electrons of a neutral gold atom. As a result of this the L→Au and X−Au vertices are donors of one and zero skeletal electrons, respectively.

Many of the gold clusters of interest have an interstitial gold atom at the center of the polyhedron formed by the peripheral gold atoms. Ten of the 11 valence electrons of this central gold atom are needed to fill its five d orbitals. Therefore an interstitial gold atom is a donor of 11−10=1 skeletal electron.

An important difference between the gold vertices L→Au and X−Au (e.g. **III**) and the B–H vertices in the deltahedral boranes (e.g **II**) is the absence of twin internal (tangential) p orbitals on the gold vertices of suitable energies to participate in surface bonding of the same kind found in globally delocalized deltahedral boranes such as $B_{12}H_{12}^{2-}$. This absence of surface bonding orbitals in icosahedral gold clusters to mix with core bonding orbitals has the consequence that both the principal core orbital corresponding to the +5 eigenvalue of the icosahedron (i.e. the S^σ orbital in the tensor surface harmonic designation outlined above) and the triply degenerate P^σ orbitals corresponding to the $+\sqrt{5}$ eigenvalue of the icosahedron (Fig. 4) remain bonding orbitals. Thus an icosahedral gold cluster has eight skeletal electrons, namely two for the single S^σ orbital and six for the triply degenerate P^σ orbitals. In the known centered icosahedral gold cluster $Au_{12}(Au)Cl_2(PMe_2Ph)_{10}^{3-}$ these eight skeletal electrons arise as follows:

10 $AuPMe_2Ph$ vertices (10)(1) =	10 electrons
2 AuCl vertices	0 electrons
Interstitial gold atom	1 electron
+3 charge on ion	−3 electrons
Total skeletal electrons in $Au_{12}AuCl_2(PMe_2Ph)_{10}^{3+}$:	8 electrons

More complicated coinage metal clusters have structures based on the linking or fusion of two or more coinage metal icosahedra (Fig. 8). The 25-atom cluster $\{[(p\text{-}MeC_6H_4)_3P]_{10}Au_{13}Ag_{12}Br_8\}^+$ has two Au-centered

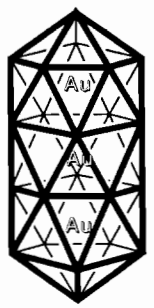

$\{[(p\text{-}MeC_6H_4)_3P]_{10}Au_{13}Ag_{12}Br_8\}^+$

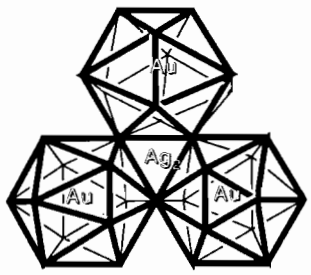

$[(p\text{-}MeC_6H_4)_3P]_{12}Au_{18}Ag_{20}Cl_{14}$

Fig. 8. Fusions of two and three icosahedra in the metal frameworks of coinage metal clusters showing the interstitial atoms.

Au_6Ag_6 icosahedra fused together by sharing one vertex [55]. The 38-atom cluster $[(p\text{-}MeC_6H_4)_3P]_{12}Au_{18}Ag_{20}Cl_{14}$ contains three Au-centered Au_6Ag_6 icosahedra fused together by sharing three corners in a triangular arrangement, thereby leading to a (3)(13) − 3 = 36 atom cluster; two more exopolyhedral Ag atoms are added to the top and the bottom Ag_3 triangles along the threefold axis (designated 'Ag_2' in Fig. 8) [56].

4. Elemental boron and boron-rich borides

The previous section discusses globally delocalized icosahedral finite molecules and ions including $B_{12}H_{12}^{2-}$ containing boron icosahedra. Such boron icosahedra can be used to construct infinite solid state structures including the allotropes of elemental boron as well as some boron-rich borides. Understanding the structure and bonding in infinite solid state structures based on icosahedral B_{12} building blocks is also relevant to understanding the icosahedral quasicrystals discussed in the next section, which are constructed from aluminum icosahedra. Note that an icosahedral B_{12} building block in which each of the twelve vertices contributes a single electron for an external two-electron two-center bond to an external group requires a total of 38 electrons distributed as follows:

Electrons for each of the 12 external bonds:	12 electrons
Electrons for the 12-center core bond of the B_{12} icosahedron:	2 electrons
Electrons for the surface bonding:	24 electrons
Total electrons required:	38 electrons

Since 12 boron atoms have a total of (12)(3) = 36 valence electrons, such an icosahedral B_{12} unit is stable as the formal dianion B_{12}^{2-}.

Elemental boron exists in a number of allotropic forms of which four (two rhombohedral forms and two tetragonal forms) are well established [5, 6, 57]. The structures of all of these allotropic forms of boron are based on various ways of joining B_{12} icosahedra using the external orbitals on each boron atom. The structures of the two rhombohedral forms of elemental boron are of interest in illustrating what can happen when icosahedra are packed into an infinite three-dimensional lattice. Note that in rhombohedral structures the local symmetry of an icosahedron is reduced from I_h to D_{3h} because of the loss of the five-fold rotation axes. The twelve vertices of an icosahedron, which are all equivalent under I_h local symmetry, are split under D_{3h} local symmetry into two non-equivalent sets of six vertices each (Fig. 9). The six rhombohedral vertices (labeled R in Fig. 9) define the directions of the rhombohedral axes. The six equatorial vertices (labeled E in Fig. 9) lie in a staggered belt around the equator of the icosahedron. The six rhombohedral and six equatorial vertices form prolate (elongated) and oblate (flattened) trigonal antiprisms, respectively.

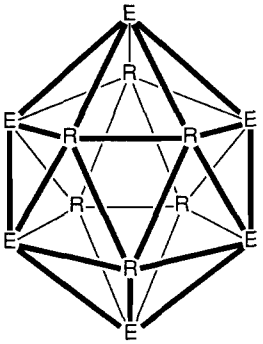

Fig. 9. The six rhombohedral (labeled R) and six equatorial (labeled E) vertices of an icosahedron.

In the simple (α) rhombohedral allotrope of boron all boron atoms are part of discrete icosahedra. In a given B_{12} icosahedron the external orbitals of the rhombohedral boron atoms (R in Fig. 9) form two-center bonds with rhombohedral boron atoms of an adjacent B_{12} icosahedron and the external orbitals of the equatorial boron atoms (E in Fig. 9) form three-center bonds with equatorial borons of two adjacent B_{12} icosahedra. The available (12)(3) = 36 electrons from an individual B_{12} icosahedron in α-rhombohedral boron are fully used as follows:

Skeletal bonding	
12-center core bond:	2 electrons
12 2-center surface bonds: (12)(2) =	24 electrons
External bonding	
(a) Rhombohedral borons:	
1/2 of six 2-center bonds: (6/2(2)) =	6 electrons
(b) Equatorial borons:	
1/3 of six 3-center bonds: (6/3)(2) =	4 electrons
Total electrons required:	36 electrons

α-Rhombohedral boron thus has a closed-shell electronic configuration.

The structure of the complicated (β) rhombohedral allotrope of boron avoids the three-center intericosahedral bonding of α-rhombohedral boron but is considerably more complicated. The structure of β-rhombohedral boron may be described as a rhombohedral packing of B_{84} polyhedral networks known as Samson complexes (Fig. 10) [58] linked by B_{10} polyhedra and an interstitial boron atom so that the fundamental structural unit is $B_{84}(B_{10})_{6/3}B = B_{105}$. The idealized isolated B_{84} Samson complexes have I_h local symmetry which is distorted to D_{3h} in the rhombohedral local environment of the lattice. Within the B_{84} Samson complex the external orbital of each of the twelve boron atoms of a central B_{12} icosahedron forms a two-center bond with the external orbital of an apical boron atom

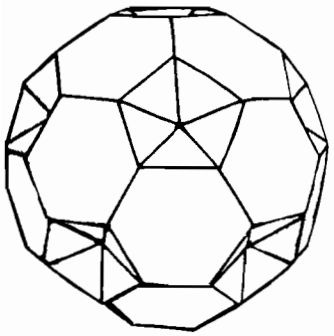

Fig. 10. A view of the surface of a Samson complex showing six of the twelve pentagonal pyramid cavities.

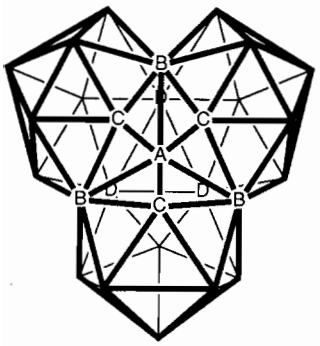

Fig. 11. The B_{28} polyhedron linking three Samson complexes in the β-rhombohedral boron structure.

of a B_6 pentagonal pyramid (i.e. a half icosahedron) leading to the $B_{12}(B_6)_{12} = B_{84}$ stoichiometry of this B_{84} Samson complex. The external surface of this B_{84} Samson complex (Fig. 10) is a B_{60} truncated icosahedron identical to the C_{60} truncated icosahedron of fullerene [59]. The B_6 pentagonal pyramids in the rhombohedral positions (see R of Fig. 9) of the central B_{12} icosahedron of the B_{84} Samson complex overlap with analogous B_6 pentagonal pyramids of adjacent B_{84} Samson complexes to form six new B_{12} icosahedral cavities. The B_6 pentagonal pyramids in the equatorial positions (see E of Fig. 9) of the central B_{12} icosahedron of the B_{84} Samson complexes each overlap with the corresponding equatorial B_6 pentagonal pyramids of two adjacent B_{84} Samson complexes by means of an additional B_{10} unit to form new polyhedra of 28 boron atoms (Fig. 11). These B_{28} units have local C_{3v} symmetry and are constructed by fusion of three icosahedra so that in each icosahedron one vertex (vertex A in Fig. 11) is shared by all three icosahedra and four vertices (B and D in Fig. 11) are each shared by two of the icosahedra so that $3(B_7B_{4/2}B_{1/3}) = B_{28}$.

In order to consider an electron counting scheme for β-rhombohedral boron, it is first necessary to consider the chemical bonding topology of the idealized B_{28} polyhedron (Fig. 11) formed by the fusion of three globally delocalized boron icosahedra. The 28 boron atoms furnish a total of $(28)(4) = 112$ valence orbitals of which 24 orbitals (one on each boron atom except for the four boron atoms labelled A and B in Fig. 11) are required for external bonding leaving $112 - 24 = 88$ atomic orbitals for the skeletal (internal) bonding. A 12-center core bond in each of the icosahedral cavities of the B_{28} polyhedron requires $(3)(12) = 36$ atomic orbitals leaving $88 - 36 = 52$ atomic orbitals for pairwise surface bonding corresponding to 26 surface bonds. Thus a closed shell electronic configuration for the B_{28} polyhedron with one electron in each external orbital is B_{28}^{2+} requiring 82 electrons as follows:

24 external two-center bonds: (24/2)(2)	24 electrons
3 12-center core bonds: (3)(2) =	6 electrons
26 surface bonds: (26)(2) =	52 electrons
Total electrons required:	82 electrons

Three boron positions (D in Fig. 11) in the B_{28} polyhedron are only partially occupied ($\sim 2/3$) because of the availability of only four valence orbitals on the interstitial boron for chemical bonding. This corresponds approximately to removing one of these boron atoms from each B_{28} polyhedron. Removal of this boron atom from the B_{28} polyhedron to give a B_{27} polyhedron removes three electrons and four orbitals. Loss of these four orbitals has the following three effects:

(i) one external bond is eliminated reducing the total required number of electrons by one;

(ii) one core bond is reduced from a 12-center bond to an 11-center bond with no effect on the required number of electrons;

(iii) one surface bond is eliminated reducing the required number of electrons by two. Thus the removal of one D vertex in the B_{28} polyhedron removes three electrons but also the need for three electrons ($3 = 1 + 0 + 2$ from (1), (2), and (3) above, respectively) so that the net charge on the species with the closed shell electronic configuration is not affected.

Additional complicating features of the structure of β-rhombohedral boron are the partial occupancy of some boron sites and the presence of interstitial boron atoms as follows [60]:

(i) three of the boron vertex sites of the B_{10} unit linking three B_6 pentagonal pyramids to form the B_{28} polyhedron, namely the vertices marked 'D' in Fig. 10, are only partially occupied (73.4%).

(ii) there is an interstitial boron atom (designated as B(15) in the structural papers) within bonding distance of six of the above partially occupied boron vertex sites corresponding approximately to an isolated tetracoordinated boron atom (i.e $(0.734)(6) = 4.4$);

(iii) there is also a partially occupied (24.8%) interstitial site in the B_{84} Samson complex.

The boron atom in the fully occupied interstitial site (B(15) in the structural papers) bonded to four boron

atoms of the B_{27} polyhedron (D in Fig. 11) has a closed shell configuration B^- (compare BH_4^- or $B(C_6H_5)_4^-$). The ~25% occupancy of the other six interstitial sites in each B_{84} Samson complex (B(16) in the structural papers) provides another $B_{1.5}$ to the fundamental structural unit. This additional $B_{1.5}$ provides an extra (1.5)(3) = 4.5 electrons without adding any new bonding orbitals since the atomic orbitals of these latter interstitial boron atoms merely increase some two-center surface bonds to three-center bonds.

All of these considerations lead to a very complicated model for the chemical bonding topology of β-rhombohedral boron. The electron counting in its fundamental $B_{104.5}$ structural unit is summarized in Table 1. The net charge of −0.5 for a 313.5 (=(3)(104.5)) valence electron structural unit can be assumed to be zero within the experimental error of partial occupancies, etc., indicating that β-rhombohedral boron, like the much simpler α-rhombohedral boron, has a closed shell electronic configuration. Note that in the lattices of both rhombohedral forms of boron, the six rhombohedral (R in Fig. 9) and six equatorial (E in Fig. 9) borons of a central B_{12} icosahedron are linked to two and three other such B_{12} icosahedra, respectively, using simple two-center and three-center chemical bonds, respectively, for α-rhombohedral boron but using B_{12} icosahedra and B_{28} polyhedra (Fig. 11), respectively, for β-rhombohedral boron.

Boron icosahedra are also found in boron-rich borides of the most electropositive metals such as lithium, sodium, magnesium and aluminium [61]. The structures of such borides are related to the alkali metal gallides discussed in the previous section. In the structures of these boron rich-borides the electropositive metals can be regarded as forming cations, e.g. Li^+, Na^+, Mg^{2+}, etc., and the boron subnetwork then has a corresponding negative charge. An important structural unit in such borides is B_{14}^{4-} which may be written more precisely as $(B_{12}^{2-})(B^-)_2$. Thus consider the magnesium boride $Mg_2B_{14} = (Mg^{2+})_2(B_{12}^{2-})(B^-)_2$ [62]. Half of the external bonds from the B_{12} icosahedra are direct bonds to other B_{12} icosahedra whereas the other half of these external bonds are to the isolated boron atoms. Closely related structures are found in $LiAlB_{14}$ [63] and the so-called '$MgAlB_{14}$'. However, '$MgAlB_{14}$' is actually $MgAl_{2/3}B_{14}$ because of partial occupancy of the aluminum sites and thus can be formulated with the same B_{14}^{2-} unit as Mg_2B_{14} [64]. A less closely related structure is $NaB_{0.8}B_{14}$, which has two types of interstitial boron atoms as well as the same B_{12}^{2-} icosahedra [65].

The lanthanides are also examples of electropositive metals that form boron-rich borides having boron subnetworks constructed from B_{12} icosahedra. An example of an extremely boron-rich metal boride is YB_{66} [66, 67]. The structure of YB_{66} is even more complicated than that of β-rhombohedral boron discussed above and has not been worked out in complete detail. The unit cell of YB_{66} has approximately 24 yttrium atoms and 1584 boron atoms. The majority of the boron atoms (1248 = (8)(156)) are contained in thirteen-icosahedron units of 156 atoms each. In such a thirteen-icosahedron unit a central B_{12} icosahedron is surrounded by 12 icosahedra leading to a B_{156} 'icosahedron of icosahedra'. The remaining boron atoms are statistically distributed in channels that result from the packing of the thirteen-icosahedron units and form non-icosahedral cages which are not readily characterized. The complexity of this structure and the uncertainty in the positions of the 'interstitial' boron atoms clearly precludes any serious attempts at electron counting.

Another interesting solid state boron compound is the refractory material boron carbide which has stoichiometries B_4C (=$B_{12}C_3$) [68] to $B_{13}C_2$ [69]. These compounds have an interesting structure in which B_{12} icosahedra are linked by planar C_2B_4 six-membered rings similar to the six-membered rings in the planar graphite (Fig. 12). The planarity of the six-membered C_2B_4 rings suggests 'benzenoid-type' aromaticity. Ad-

TABLE 1. Boron and electron counting in β-rhombohedral boron

	Boron atoms	Net charge
Central B_{12} icosahedron	12	−2
6/2 Rhombohedrally located peripheral B_{12} icosahedra		
(6/2)(12) =	36	
(6/2)(−2) =		−6
6/3 Equatorially located peripheral B_{27} polyhedra		
(6/3)(27) =	54	
(6/3)(+2) =		+4
1 B(15) interstitial boron atom	1	−1
(0.25)(6) = 1.5 B(16) interstitial boron atoms		
(1.5)(1) =	1.5	
(1.5)(+3) =		+4.5
Total boron atoms and overall net charge	104.5	−0.5

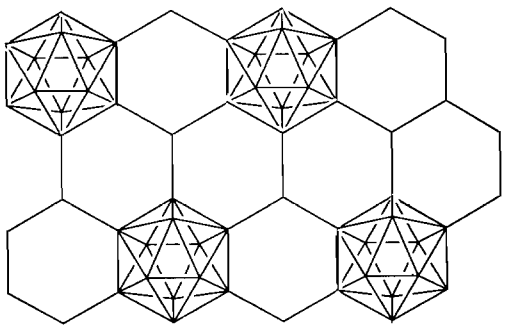

Fig. 12. A hexagonal layer in $B_{12}C_3$ or $B_{13}C_2$ showing the fusion of the B_4C_2 planar hexagons to the B_{12} icosahedra.

ditional carbon (in $B_{12}C_3$) or boron (in $B_{13}C_2$) atoms link the carbon atoms to form allene-like C_3 or CBC chains, respectively, in directions perpendicular to the planes of the C_2B_4 rings. The combination of the very stable 'aromatic' hexagonal C_2B_4 rings fused to the likewise very stable B_{12} icosahedra can account for the observed stability and strength of the $B_{12}C_3$ and $B_{13}C_2$ structures including the extreme hardness and high melting points of these boron carbides.

5. Aluminum icosahedra in quasicrystals

The previous sections of this paper discuss borane anions, elemental boron structures, and boron-rich borides having structures containing B_{12} icosahedra and alkali metal gallides having Ga_{12} icosahedra. Aluminum compounds containing Al_{12} icosahedra are much rarer although i-$Bu_{12}Al_{12}^{2-}$ isoelectronic with $B_{12}H_{12}^{2-}$ has recently been reported [70] as a low yield product from the reduction of i-Bu_2AlCl with potassium metal. However, of much greater interest has been the discovery of aluminum alloys exhibiting diffraction patterns with apparently sharp spots containing the five-fold symmetry axes characteristic of icosahedra [71, 72]. This discovery raises a crystallographic dilemma since the sharpness of the diffraction peaks suggests long range translational order, as in periodic crystals, but five-fold axes are incompatible with such periodicity. Such materials are described as quasicrystals [73, 74], which are defined to have delta-functions in their Fourier transform but local point symmetries incompatible with periodic order. The structures of these materials may be regarded as three-dimensional analogues of Penrose tiling [75–78] which is a geometric structure exhibiting five-fold symmetries and Bragg diffraction. Locations of atoms in quasicrystals requires the use of six-dimensional crystallography [79, 80] in which the atoms correspond to three-dimensional hypersurfaces in six-dimensional periodic lattices. For this reason the chemical structures of quasicrystals are not readily described in ways familiar to chemists. Chemically based models for quasicrystal structures are therefore more readily developed by first considering closely related true crystalline materials and then introducing appropriate perturbations destroying the periodic translational order but retaining the long range translational and orientational order characteristic of quasicrystals.

There are several types of icosahedral quasicrystals with diverse compositions [81]. The most important types, including the following, contain large amounts of aluminum:

(i) the i(Al-Mt) class (Mt = transition metal) including (i-$(Al_{80}Mn_{20})$, i-$(Al_{74}Mn_{20}Si_6)$ [82, 83], i-$(Al_{79}Cu_{17}Ru_4)$ [84];

(ii) the i-(AlZnMg) class including i-$(Al_{25}Zn_{38}Mg_{37})$ [85], i-$(Al_{44}Zn_{15}Cu_5Mg_{36})$ [86] and i-$(Al_{60}Cu_{10}Li_{30})$ [87]. The relatively large amounts of aluminum in all of these phases suggests comparison of the structures of these materials with those of the icosahedral boron and gallium derivatives discussed above.

Consider the i-$(Al_{60}Cu_{10}Li_{30})$ system and related alloys containing aluminum, lithium, and copper and/or zinc, which have been discussed in detail by Audier *et al.* [88]. This system is significant since there are crystalline phases similar to the so-called T2 icosahedral quasicrystalline phases. The atom positions in the cubic R phase of approximate Al_5CuLi_3 stoichiometry are known so that the structure of this phase can provide some insight into the structure of the closely related T2 icosahedral phase of approximate stoichiometry $Al_{0.570}Cu_{0.108}Li_{0.322}$. Here a model for the chemical bonding topology in crystalline R-Al_5CuLi_3 is summarized; further details of this model are summarized elsewhere [89].

Audier *et al.* have described a polyhedral shell structure for R-Al_5CuLi_3 consisting of the following layers:

(a) a central $(Al,Cu)_{12}$ icosahedron;

(b) an Li_{20} regular dodecahedron with the Li positions above the faces of the central $(Al,Cu)_{12}$ icosahedron (layer a);

(c) a larger $(Al,Cu)_{12}$ icosahedron formed from the external orbitals of the central $(Al,Cu)_{12}$ icosahedron (layer a) so that its atoms lie above the twelve faces of the Li_{20} dodecahedron;

(d) An $(Al,Cu)_{60}$ truncated icosahedron (Fig. 13) distorted from I_h local symmetry to O_h symmetry so that 12 vertices are of one type (circled in Fig. 13) and 48 vertices are of another type (not circled in Fig. 13). The atoms of this truncated icosahedron lie above the midpoints of the faces of the omnicapped dodecahedron (Fig. 3) formed by combining the Li_{20} dodecahedron (layer b) with the larger $(Al,Cu)_{12}$ icosahedron (layer c).

The (Al–Cu) subskeleton (layers a+c+d discussed above) in R-Al_5CuLi_3 forms a lattice containing 84

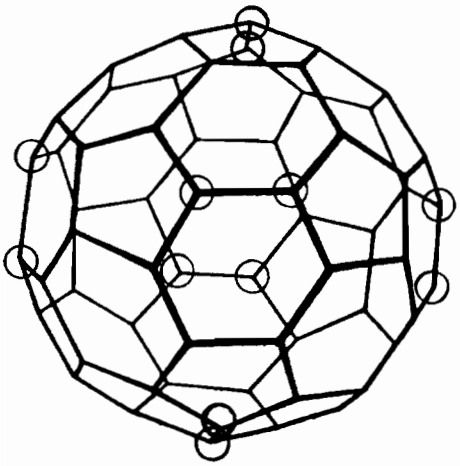

Fig. 13. The two different types of vertices in the $(Al,Cu)_{60}$ truncated icosahedron distorted from I_h to O_h symmetry found in the structure of cubic R-Al_5CuLi_3.

vertex Samson complexes (Fig. 10) identical to the B_{84} Samson complex found in the β-rhombohedral boron lattice discussed in the previous section. However, the packing of the $(Al,Cu)_{84}$ Samson complexes in the R-Al_5CuLi_3 lattice is totally different from the packing of the B_{84} Samson complexes in β-rhombohedral boron. The Al–Cu subskeleton of the R-Al_5CuLi_3 lattice thus consists of a CsCl-type cubic packing of the $(Al,Cu)_{84}$ Samson complexes so that each atom of the peripheral $(Al,Cu)_{60}$ truncated icosahedron of the $(Al,Cu)_{84}$ Samson complex is shared with an adjacent Samson complex in one of the following two ways:

(i) the six edges connecting the six pairs of circled vertices in Fig. 13 lie in the faces of a cube and are shared with the corresponding edge of the adjacent Samson complex in the adjacent cube sharing the face containing the edge in question;

(ii) the eight hexagonal faces of the peripheral $(Al,Cu)_{60}$ truncated icosahedron not containing any of the circled vertices in Fig. 13 are shared with the corresponding faces of the adjacent Samson complex in the cube sharing the vertex lying at the end of the body diagonal of the original cube containing the midpoint of the hexagonal face in question.

The fundamental structural unit of the (Al,Cu) subskeleton of R-Al_5CuLi_3 thus is $(Al,Cu)_{54} = (Al,Cu)_{12} + (Al,Cu)_{12} + (Al,Cu)_{60/2}$ corresponding, respectively, to the layers a+c+d discussed above. In addition to the 20 lithium atoms in layer b, additional lithium atoms (layer e) are located above the pentagonal faces of the peripheral truncated icosahedra, which, because of the way that the truncated icosahedra are linked, simultaneously cap the pentagonal faces of two adjacent truncated icosahedron sharing an edge (sharing method 1 above). The sum of the number of atoms in layers a through e, respectively, in this model is $(Al,Cu)_{12} + Li_{20} + (Al,Cu)_{12} + (Al,Cu)_{60/2} + Li_{12/2} = (Al,Cu)_{54}Li_{26}$ corresponding to an (Al+Cu)/Li ratio of 2.08 in close agreement with 2.12 implied by the $Al_{0.570}Cu_{0.108}Li_{0.322}$ stoichiometry.

Now consider the electron counting in R-Al_5CuLi_3. In the (Al,Cu) subskeleton the aluminum and copper atoms can function as donors of three and one, electrons, respectively, assuming in the case of copper a stable d^{10} configuration corresponding to Cu^+. The lithium atom is a one-electron donor by ionization to Li^+. This combined with the $Al_{0.570}Cu_{0.108}Li_{0.322}$ stoichiometry leads to an $Al_{45}Cu_9^{26-}$ fundamental Samson complex structural unit corresponding to (45)(3)+(9)(1)+26=170 electrons. In addition, application of the same model to the cubic R phase of the Al–Cu–Li–Mg alloy of stoichiometry $Al_{0.52}Cu_{0.15}Li_{0.25}Mg_{0.08}$ leads to the stoichiometry $Al_{42}Cu_{12}Li_{20}Mg_6 = Al_{42}Cu_{12}^{32-}$ for the fundamental Samson complex structural unit also corresponding to (42)(3)+(12)(1)+32=170 skeletal electrons. This suggests that 170 electrons is a 'magic number' for the 54-atom Samson complex structural unit of cubic crystalline aluminum alloy phases closely related to the icosahedra quasicrystals of the i-(AlZnMg) class. This model assumes that the aluminum and copper atoms in these structures occupy the vertices of the Samson complexes (layers a, c and d) and the more electropositive metals (Li and Mg) occupy interstitial positions (layers b and e).

The topology of the 84-atom Samson complex (Fig. 10) and the linkages of such complexes in a CsCl-type cubic lattice in R-Al_5CuLi_3 are consistent with the observed 170 skeletal electrons corresponding to a closed shell electronic configuration with delocalized bonding in polyhedral cavities of the following two types:

(i) the central $(Al,Cu)_{12}$ icosahedron (layer a) having the required 26 skeletal electrons for globally delocalized chemical bonding topology;

(ii) the twelve pentagonal pyramid $(Al,Cu)^a$-$(Al,Cu)^b_{5/2}$ cavities (layers c and d) in which $(Al,Cu)^a$ refers to the single apical atom and $(Al,Cu)^b_{5/2}$ refers to the five basal atoms; each of the basal atoms is part of two different pentagonal pyramid cavities forming parts of different Samson complexes and thus has only two internal orbitals to contribute to the skeletal bonding of a given pentagonal pyramid cavity. In Fig. 10 six of the total of 12 pentagonal pyramid cavities can be seen on the surface of the Samson complex.

The *nido* bonding [90] in a pentagonal pyramid leading to $2n+4=16$ skeletal electrons and eight bonding orbitals requires (6)(3)=18 internal orbitals. However, in the pentagonal pyramid cavities in the Samson complex in the R-Al_5CuLi_3 structure there are only 3+(5)(2)=13 internal orbitals. For this reason only one five-center core bond and four two-center surface

TABLE 2. Electron and orbital counting in a Samson complex structural unit in R-Al_5CuLi_3

	Total electrons	Total orbitals
(A) 1 central $(Al,Cu)_{12}$ icosahedron (layer a)		
Core bonding: (2 electrons; 12 orbitals)	2	12
Surface bonding: ((12)(2) = 24 electrons; 24 orbitals)	24	24
(B) 12 two-center bonds between the external orbitals of the central $(Al,Cu)_{12}$ icosahedron (layer a) and the $(Al,Cu)_{12}$ icosahedron in the next layer (layer b): (2 electrons; 2 orbitals) × 12	24	24
(C) 12 $(Al,Cu)^a(Al,Cu)^b_{5/2}$ pentagonal pyramid cavities		
Core bonding (5 center): (2 electrons, 5 orbitals) × 12 =	24	60
Surface bonding: (4)(2) = (8 electrons, 8 orbitals) × 12 =	96	96
Total electrons and orbitals per $(Al,Cu)_{12}(Al,Cu)_{12}(Al,Cu)_{60/2}$ Samson complex	170	216

bonds are possible using these 13 internal orbitals leading to 10 rather than 16 skeletal electrons for each pentagonal pyramid. The details of the chemical bonding topology for an $(Al,Cu)_{12}(Al,Cu_{12})(Al,Cu)_{60/2}$ Samson complex are outlined in Table 2; this chemical bonding topology can lead to the observed 170 electrons while using the available $4(12+12+60/2) = 216$ valence orbitals of the sp^3 manifolds of the 54 vertex atoms.

The above discussion considers a model for the structure of the crystalline cubic R-Al_5CuLi_3. Now consider possible perturbations in this model to give the quasicrystal T2-Al_5CuLi_3. In this connection the 54-vertex Mackay icosahedron (Fig. 14) [91] appears as a structural unit in certain quasicrystals [92]. The Mackay icosahedron has a shell structure consisting of the following layers:

(a) a central icosahedron (not visible in Fig. 14);

(b) a larger icosahedron formed from the external orbitals of the atoms in the central icosahedron (layer a) overlapping with an additional set of twelve atoms (black circles in Fig. 14);

(c) a 30-vertex icosidodecahedron formed by placing atoms above each of the 30 edges of the larger icosahedron (layer b). Layer c is shown as white circles in Fig. 14.

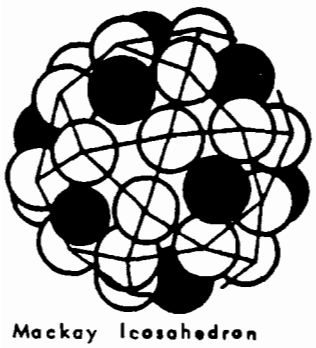

Fig. 14. A view of the surface of a Mackay icosahedron showing the vertices of the large icosahedron (layer b) as black circles and the vertices of the icosidodecahedron (layer c) as white circles. The vertices of the central icosahedron (layer a) are not visible.

Layers a and b of the Mackay icosahedron are identical to the first two layers of the Samson complex (i.e. layers a and c in the Audier model discussed above). However, the outer icosidodecahedron layer of the Mackay icosahedron (layer c) has exactly half of the number of atoms of the outer truncated icosahedron in the Samson complex. Furthermore, the packing of the Samson complexes into the R-Al_5CuLi_3 lattice results in each of the peripheral truncated icosahedron atoms being shared between exactly two adjacent complexes so that a single Samson complex structural unit has the same 54 atoms as a corresponding Mackay icosahedron. This suggests a very close relationship between the packing of Samson complexes in the R-Al_5CuLi_3 crystal and a possible packing of Mackay icosahedra in a T2-Al_5CuLi_3 quasicrystal. In fact a concerted 90° rotation about a tangential axis of each of the 30 edges connecting pairs of pentagonal faces in the peripheral truncated icosahedron in each Samson complex of the R-Al_5CuLi_3 crystalline lattice converts a lattice of 54-atom Samson complexes into a lattice of 54-atom Mackay icosahedra. This type of process may be crucial in converting crystals built from icosahedral building blocks to quasicrystals and resembles 'martensitic' transformations such as those found in A-15 superconductors [93].

6. Icosahedral and cuboctahedral polyoxometallates

The above sections of this paper have discussed structures containing cluster icosahedra, i.e. structures having atoms at the vertices of an icosahedron with

some type of chemical bonding, generally delocalized bonding between the vertex atoms. There is also a possibility of structures containing coordination icosahedra, namely structures of the type ML_{12} in which a central atom M is surrounded by 12 ligands L at the vertices of an icosahedron. Such a structure, at least with covalent M–L bonds, requires a manifold of 12 valence orbitals for the central atom M, which is not possible if the metal atom uses only the nine-orbital sp^3d^5 manifold. For this reason a coordination icosahedron in an ML_{12} complex requires a central atom M which has accessible f orbitals thereby restricting coordination icosahedra to lanthanide and actinide chemistry. In addition, the steric requirements for surrounding a central atom with 12 ligands are substantial suggesting that coordination icosahedra will only occur in special situations in which the twelve ligands L have unusually low steric requirements and where external features of the structure force 12 ligands in icosahedral coordination around a central atom. All of these requirements are met in the icosahedral Silverton polyoxometallates having the general formula $M^{IV}Mo_{12}O_{42}^{8-} = M^{IV}(MoO^t_2O^b_{1/2}O^i_{3/3})_{12}^{8-}$ (M = Ce, Th, U; O^t = terminal oxygen atoms; O^b = atoms bridging the polyhedral surface; O^i = internal oxygen atoms, i.e. oxygen atoms coordinated icosahedrally to the central lanthanide or actinide) [17]. These icosahedral polyoxometallates are depicted schematically in Fig. 15.

The chemical properties of polyoxometallates containing twelve molybdenum or tungsten atoms are closely related to the nature of the 12-vertex polyhedron formed by these metal atoms and the possibilities for delocalized metal–metal interactions through M–O–M bridges. Thus a characteristic of many, but not all, of such polyoxometallates is their reducibility to highly colored mixed oxidation state derivatives [94], e.g. 'molybdenum blues' and 'tungsten blues'. The redox properties of these polyoxometallates make them important as catalysts for a number of oxidation and dehydrogenation reactions of organic substrates [95, 96].

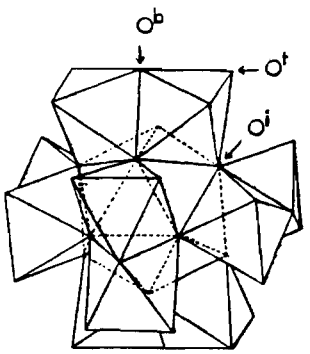

Fig. 15. The structure of the Silverton icosahedral polyoxometallates $M^{IV}M_{12}O_{42}^{8-}$ showing the three types of oxygen atoms (O^t, O^b, and O^i).

Several efforts have been made to relate the redox properties of early transition metal polyoxometallates to their structures. Pope [97] first noted that the reducibility of early transition metal polyoxometallates requires the presence of MO_6 octahedra in which only one of the six oxygen atoms is a terminal oxygen atom. Such an MO_6 octahedron can be related to mononuclear L_5MO species [98] in which there is an essentially nonbonding metal d orbital to receive one or two electrons. Nomiya and Miwa [99] developed the idea of a structural stability index based on interpenetrating loops –O–M–O–M–O– around the polyoxometallate cage and suggested the analogy of closed loops of this type to macrocyclic π-bonding systems. The relationships of such macrocyclic π-bonding systems to aromaticity such as that found in certain organic annulenes suggests that readily reducible polyoxometallates have some kind of aromatic properties. Thus the ready one-electron reduction of a colorless to yellow polyoxomolybdate or polyoxotungstate to a highly colored mixed valence 'blue' may be viewed as analogous to the one-electron reduction of benzenoid hydrocarbons such as naphthalene or anthracene to the highly colored corresponding radical anion.

The polyoxometallates of interest consist of closed networks of MO_6 octahedra in which M is a d^0 early transition metal such as V(V), Nb(V), Mo(VI) or W(VI). These networks may be described by the large polyhedron formed by the metal atoms M as vertices. In general the edges of this macropolyhedron are M–O–M bridges and with rare exceptions there is no metal–metal (M–M) bonding. The oxygen atoms in these structures are of three types:

(i) *terminal or external oxygen atoms* (designated as O^t) which are multiply bonded to the metal (one σ and up to two orthogonal π bonds) and directed away from the macropolyhedral surface;

(ii) *bridging or surface oxygen atoms* (designated as O^b) which form some or all of the macropolyhedral edges;

(iii) *internal oxygen atoms* (designated as O^i) which are directed towards the center of the macropolyhedron.

The metal vertices of the macropolyhedron may be classified as $(\mu_n\text{-O})_5MO$ or *cis*-$(\mu_n\text{-O})_4MO_2$ vertices depending on the number and locations of the terminal oxygen atoms (i.e. O = terminal oxygen atoms only). In the *cis*-$(\mu_n\text{-O})_4MO_2$ vertices all nine orbitals of the sp^3d^5 manifold of M are used for the σ and π bonding to the two terminal oxygen atoms and σ bonding to the four bridging and internal oxygen atoms leaving no orbitals for direct or indirect overlap with other metal vertices of the metal macropolyhedron. The *cis*-$(\mu_n\text{-O})_4MO_2$ vertices in polyoxometallates correspond to the saturated CH_2 vertices in cyclohexanes and other cycloalkanes. In the $(\mu_n\text{-O})_5MO$ vertices (IV) only eight

of the nine orbitals of the sp^3d^5 manifold of M can be used for σ and π bonding to the single terminal oxygen atom and σ bonding to the five bridging and internal oxygen atoms leaving one non-bonding d orbital (d_{xy} if the M≡O(terminal) axis is the z axis). Thus an $(\mu_n\text{-O})_5\text{MO}$ vertex (IV) with a nominally non-bonding d_{xy} orbital in a polyoxometallate is analogous to an unsaturated CH vertex with a non-bonding p orbital in a planar aromatic hydrocarbon such as benzene.

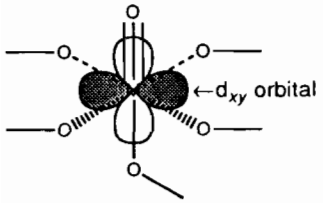

IV

These elementary considerations suggest that early transition metal polyoxometallates constructed from $(\mu_n\text{-O})_5\text{MO}$ units (IV) have the potential for electron delocalization based on overlap of the non-bonding d_{xy} orbitals. However, since these polyoxometallates are constructed from macropolyhedra having relatively long M–O–M edges rather than normal metal polyhedra having the much shorter M–M edges, the direct overlap of the d_{xy} orbitals on different metal atoms is negligible. Instead the metal–metal interactions using these metal d_{xy} orbitals must also involve the orbitals of the oxygen atoms in the M–O–M bridges and thus resemble the exchange coupling between metal atoms in antiferromagnetic systems [100]. Thus the electron delocalization in polyoxometallates having $(\mu_n\text{-O})_5\text{MO}$ vertices is based on indirect M–O–M interactions using the metal d_{xy} and appropriate bridging oxygen p orbitals rather than direct M–M interactions such as those found in metal clusters. For this reason electron delocalization in reduced polyoxometallates is much weaker than that in either planar aromatic hydrocarbons or deltahedral boranes and carboranes. This weaker interaction translates to a much lower value of the parameter β in eqns. (16) and (17).

The non-bonding d_{xy} orbitals of the $(\mu_n\text{-O})_5\text{MO}$ vertices (IV) in the reducible early transition metal polyoxometallates have two orthogonal nodes and thus have improper four-fold symmetry. Matching this four-fold orbital symmetry with the overall macropolyhedral symmetry requires macropolyhedra in which a C_4 axis passes through each vertex. A true three-dimensional polyhedron having C_4 axes passing through each vertex can have only O or O_h symmetry (the only point groups with multiple C_4 axes). The only two polyhedra having less than 15 vertices meeting these conditions are the regular octahedron and the cuboctahedron. It is therefore not surprising that these two polyhedra form the basis of the specific early transition metal polyoxometallate structures containing only $(\mu_n\text{-O})_5\text{MO}$ vertices (IV), which are type I structures in the Pope nomenclature [98].

These structures containing only $(\mu_n\text{-O})_5\text{MO}$ vertices (III) can be contrasted with the non-reducible polyoxometallate structures containing only *cis*-$(\mu_n\text{-O})_4\text{MO}_2$ vertices (type III structures in the Pope nomenclature) [97]. These structures are necessarily more open since only four of the six oxygens of the MO_6 octahedra can be bridging oxygens. The most stable polyoxometallate structure with only (*cis*-$(\mu_n\text{-O})_4\text{MO}_2$ vertices is the icosahedral Silverton structure (Fig. 15) in which the central metal atom forms an MO_{12} icosahedron with the interior oxygen atoms. The central metal is twelve-coordinate and therefore is a large tetravalent lanthanide or actinide with accessible f orbitals. An icosahedron can be decomposed into five equivalent octahedra by partitioning the 30 edges of the icosahedron into five equivalent sets of six edges each so that the midpoints of the edges in each set form a regular octahedron [26]. The vertices of the O^b_6 large octahedron in $MMo_{12}O_{42}^{8-}$ are located above the midpoints of the six edges in one of these octahedral sets of six icosahedral edges (Fig. 15).

The Silverton icosahedral polyoxometallates $MMo_{12}O_{42}^{8-}$ are non-reducible type III structures in the Pope nomenclature [97] and may be contrasted with the Keggin cuboctahedral polyoxometallates $XM_{12}O_{40}^{n-} = (MO^tO^b_{4/2}O^i_{1/3})_{12}X^{n-}$, where $n = 3$ to 7; M = Mo, W; X = B, Si, Ge, P, Fe^{III}, Co^{II}, Cu^{II}, etc., which are reducible type I structures in the Pope nomenclature. The cuboctahedral Keggin structure may be regarded as an example of a binodal orbital aromatic system since the non-bonding d_{xy} orbital of the $(\mu_n\text{-O})_5\text{MO}$ vertex has two nodes (see structure IV). The positive eigenvalues in the spectrum of the cuboctahedron (Fig. 4) corresponding to the overlap topology of the d_{xy} orbitals in the Keggin structure are the non-degenerate +4 and the triply degenerate +2. The highly positive non-degenerate +4 eigenvalue corresponds to a highly bonding molecular orbital, which can accommodate the first two electrons upon reduction of the initially d^0 $XM_{12}O_{40}^{n-}$. The reported [101, 102] diamagnetism of the two-electron reduction products of the $PW_{12}O_{40}^{3-}$, $SiW_{12}O_{40}^{4-}$ and $[(H_2)W_{12}O_{40}]^{6-}$ anions is in accord with the two electrons being paired in this lowest lying molecular orbital.

The concept of binodal aromaticity in reduced early transition metal polyoxometallates may be related to their classification as mixed valence compounds. Robin and Day [103] classify mixed valence compounds into the following three classes:

Class I: fully localized corresponding to an insulator in an infinite system;

Class II: partially delocalized corresponding to a semiconductor in an infinite system;

Class III: completely delocalized corresponding to a metal in an infinite system.

ESR studies on the one-electron reduced polyoxometallates $XM_{12}O_{40}^{n-}$ suggest class II mixed valence species [104, 105]. Although such species are delocalized at accessible temperatures they behave as localized systems at sufficiently low temperatures similar to semiconductors. This is in accord with the much smaller overlap (i.e. lower β in eqns. 16 and 17) of the metal d_{xy} orbitals associated with binodal orbital aromaticity as compared with the boron sp hybrid anodal internal orbitals in the deltahedral boranes $B_nH_n^{2-}$ or the carbon uninodal p orbitals in benzene.

References

1 R. B. King, in M. Gielen (ed.), *Advances in Dynamic Stereochemistry,* Vol. 2, Freund, Tel Aviv, Israel, 1988, pp. 1–36.
2 F. A. Cotton, *Chemical Applications of Group Theory,* Wiley, New York, 1971.
3 E. L. Muetterties (ed.), *Boron Hydride Chemistry,* Academic Press, New York, 1975.
4 R. N. Grimes, *Carboranes,* Academic Press, New York, 1970.
5 J. L. Hoard and R. E. Hughes, in E. L. Muetterties (ed.), *The Chemistry of Boron and its Compounds,* Wiley, New York, 1967, pp. 25–154.
6 D. Emin, T. Aselage, C. L. Beckel, I. A. Howard and C. Wood (eds.), *Boron-Rich Solids,* American Institute of Physics Conference Proceedings 140, American Institute of Physics, New York, 1986.
7 D. Levine and P. J. Steinhardt, *Phys. Rev. Lett., 53* (1984) 2477.
8 D. Levine and P. J. Steinhardt, *Phys. Rev. B, 34* (1986) 596.
9 M. Audier, C. Janot, M. de Boissieu and B. Dubost, *Philos. Mag., B60* (1989) 437.
10 R. B. King, *Inorg. Chim. Acta, 181* (1991) 217.
11 C. Belin, *Acta Crystallogr., Sect. B, 37* (1981) 2060.
12 C. Belin, *Acta Crystallogr., Sect. B, 36* (1980) 1339.
13 J. L. Vidal and J. M. Troup, *J. Organomet. Chem., 213* (1981) 351.
14 D. F. Rieck, R. A. Montag, T. S. McKechnie and L. F. Dahl, *J. Am. Chem. Soc., 108* (1986) 1330.
15 C. E. Briant, B. R. C. Theobald, J. W. White, L. K. Bell, D. M. P. Mingos and A. J. Welch, *Chem. Commun.,* (1981) 201.
16 B. K. Teo and H. Zhang, *J. Cluster Sci., 1* (1990) 155.
17 M. T. Pope, *Heteropoly and Isopoly Oxometallates,* Springer, Berlin, 1983.
18 R. B. King, *Inorg. Chem., 28* (1989) 2796.
19 F. J. Budden, *The Fascination of Groups,* Cambridge University Press, London, 1972.
20 J. K. G. Watson, *Mol. Phys., 21* (1971) 577.
21 D. Gorenstein, *Finite Groups,* Harper and Row, New York, 1968.
22 B. Grünbaum, *Convex Polytopes,* Interscience, New York, 1967.
23 T. Janssen, *Crystallographic Groups,* North Holland, Amsterdam, 1973, p. 7.
24 G. Pólya, *Acta Math., 68* (1937) 145.
25 N. G. Debruin, in E. F. Bechenback (ed.), *Applied Combinatorial Mathematics,* Wiley, New York, 1964.
26 R. B. King and D. H. Rouvray, *Theor. Chim. Acta, 69* (1986) 1.
27 E. L. Muetterties and W. H. Knoth, *Polyhedral Boranes,* Marcel Dekker, New York, 1968.
28 R. B. King and A. J. W. Duijvestijn, *Inorg. Chim. Acta, 178* (1990) 55.
29 F. Klanberg and E. L. Muetterties, *Inorg. Chem., 5* (1966) 1955.
30 W. N. Lipscomb, *Science, 153* (1966) 373.
31 N. L. Biggs, *Algebraic Graph Theory,* Cambridge University Press, London, 1974, p. 9.
32 K. Ruedenberg, *J. Chem. Phys., 22* (1954) 1878.
33 H. H. Schmidtke, *J. Chem. Phys., 45* (1966) 3920.
34 I. Gutman and N. Trinajstić, *Topics Curr. Chem., 42* (1973) 49.
35 R. B. King and D. H. Rouvray, *J. Am. Chem. Soc., 99* (1977) 7834.
36 R. B. King, *Theor. Chim. Acta, 44* (1977) 223.
37 R. B. King, *J. Math. Chem., 1* (1987) 249.
38 K. Wade, *Chem. Commun.,* (1971) 792.
39 K. Wade, *Adv. Inorg. Chem. Radiochem., 18* (1966) 1.
40 R. J. Wilson, *Introduction to Graph Theory,* Oliver and Boyd, Edinburgh, 1972, p. 16.
41 R. B. King, in R. B. King (ed.), *Chemical Applications of Topology and Graph Theory,* Elsevier, Amsterdam, 1983, pp. 99–123.
42 R. B. King, in J. F. Liebman and A. Greenberg (eds.), *Molecular Structure and Energetics,* Verlag Chemie, Deerfield Beach, FL, 1986, pp. 123–148.
43 R. B. King, *J. Comput. Chem., 8* (1987) 341.
44 R. Hoffmann and W. N. Lipscomb, *J. Chem. Phys., 36* (1962) 2179.
45 A. J. Stone, *Polyhedron, 3* (1984) 1299.
46 A. J. Stone and D. Wales, *Mol. Phys., 61* (1987) 747.
47 R. J. Johnston and D. M. P. Mingos, *Polyhedron, 5* (1986) 2059.
48 P. Brint, J. P. Cronin, E. Seward and T. Whelan, *J. Chem. Soc., Dalton Trans.* (1983) 975.
49 C. Belin and R. G. Ling, *J. Solid State Chem., 48* (1983) 40.
50 A. Ceriotti, F. Demartin, B. T. Heaton, P. Ingallina, G. Longoni, M. Manassero, M. Marchionna and N. Masciocchi, *Chem. Commun.,* (1989) 786.
51 V. G. Albano, F. Demartin, M. C. Iapalucci, G. Longoni, A. Sironi and V. Zanotti, *Chem. Commun.,* (1990) 547.
52 V. G. Albano, A. Ceriotti, P. Chini, G. Ciani, S. Martinengo and W. M. Anker, *Chem. Commun.,* (1975) 859.
53 R. S. Nyholm, *Proc. Chem. Soc.,* (1961) 273.
54 P. Pyykkö and J.-P. Desclaux, *Acc. Chem. Res., 12* (1979) 276.
55 B. K. Teo, H. Zhang and X. Shi, *Inorg. Chem., 29* (1990) 2083.
56 B. K. Teo, M. Hong, H. Zhang, D. Huang and X. Shi, *Chem. Commun.,* (1988) 204.
57 W. N. Lipscomb and D. Britton, *J. Chem. Phys., 33* (1960) 275.
58 L. Pauling, *Phys. Rev. Lett., 58* (1987) 365.
59 H. W. Kroto, A. W. Allof and S. P. Balin, *Chem. Rev., 91* (1991) 1213.
60 B. Callmer, *Acta Crystallogr., Sect. B, 33* (1977) 1951.
61 R. Naslain, A. Guette and P. Hagenmuller, *J. Less-Common Met., 47* (1976) 1.
62 A. Guette, M. Barret, R. Naslain, P. Hagenmuller, L. E. Tergenius and T. Lundström, *J. Less-Common Met., 82* (1981) 325.

63 I. Higashi, *J. Less-Common Met., 82* (1981) 317.
64 V. I. Matkovich and J. Economy, *Acta Crystallogr., Sect. B, 26* (1969) 616.
65 R. Naslain and J. S. Kasper, *J. Solid State Chem., 1* (1970) 150.
66 S. M. Richards and J. S. Kasper, *Acta Crystallogr., Sect. B, 25* (1969) 257.
67 J. S. Kasper, *J. Less-Common Met., 47* (1976) 17.
68 K. H. Clark and J. L. Hoard, *J. Am. Chem. Soc., 65* (1943) 2115.
69 G. Will and K. H. Kossobutzki, *J. Less-Common Met., 44* (1976) 87.
70 W. Hiller, K.-W. Klinkhammer, W. Uhl and J. Wagner, *Angew. Chem., Int. Ed. Engl., 30* (1991) 179.
71 D. Shechtman, I. Blech, D. Gratias and J. W. Cahn, *Phys. Rev. Lett., 53* (1984) 1951.
72 D. Shechtman and I. A. Blech, *Metall. Trans., 16A* (1985) 1005.
73 D. Levine and P. J. Steinhardt, *Phys. Rev. Lett., 53* (1984) 2477.
74 D. Levine and P. J. Steinhardt, *Phys. Rev. B, 34* (1986) 596.
75 N. de Bruijn, *Ned Akad., Weten. Proc. Ser. A., 43* (1981) 39.
76 N. de Bruijn, *Ned Akad., Weten. Proc. Ser. A, 43* (1981) 53.
77 A. L. Mackay, *Sov. Phys. Crystallogr., 26* (1981) 517.
78 A. L. Mackay, *Phys. Status Solidi A, 114* (1982) 609.
79 V. Elser and C. L. Henley, *Phys. Rev. Lett., 55* (1985) 2883.
80 P. Bak, *Phys. Rev. Lett., 56* (1986) 861.
81 C. L. Henley, *Comments Cond. Mat. Phys., 13* (1987) 59.
82 P. Guyot and M. Audier, *Philos. Mag., B52* (1985) L15.
83 L. A. Bendersky and M. J. Kauffman, *Philos. Mag., B53* (1986) L75.
84 P. A. Bancel and P. A. Heiney, *Phys. Rev. B, 33* (1986) 7917.
85 R. Ramachandrarao and G. V. S. Sastry, *Pramana, 25* (1985) L225.
86 N. K. Mukhopadhyay, G. N. Subbanna, S. Ranganathan and K. Chattopadyay, *Scr. Metall., 20* (1986) 525.
87 P. Sainford, B. Dubost and A. Dubus, *C. R. Acad. Sci. Paris, 301* (1985) 689.
88 M. Audier, C. Janot, M. de Boissieu and B. Dubost, *Philos. Mag., B60* (1989) 437.
89 R. B. King, *Inorg. Chim. Acta, 181* (1991) 217.
90 R. Rudolph and W. R. Pretzer, *Inorg. Chem., 11* (1971) 1974.
91 A. L. Mackay, *Acta Crystallogr., 15* (1962) 916.
92 P. Guyot, M. Audier and R. Lequette, *J. Phys. (Paris), 47* (1986) C3.
93 R. Madar, J. P. Senateur and R. Fruchart, *J. Solid State Chem., 28* (1979) 59.
94 R. I. Buckley and R. J. H. Clark, *Coord. Chem. Rev., 65* (1985) 167.
95 E. Papaconstantinou, D. Dimotkali and A. Politou, *Inorg. Chim. Acta, 43* (1980) 155.
96 C. L. Hill and D. A. Bouchard, *J. Am. Chem. Soc., 107* (1985) 5148.
97 M. T. Pope, *Inorg. Chem., 11* (1972) 1973.
98 C. J. Ballhausen and H. B. Gray, *Inorg. Chem., 1* (1962) 111.
99 K. Nomiya and M. Miwa, *Polyhedron, 3* (1984) 341.
100 C. J. Cairns and D. H. Busch, *Coord. Chem. Rev., 69* (1986) 1.
101 R. A. Prados and M. T. Pope, *Inorg. Chem., 15* (1976) 2547.
102 G. M. Varga, Jr., E. Papaconstantinou and M. T. Pope, *Inorg. Chem., 9* (1970) 662.
103 M. B. Robin and P. Day, *Adv. Inorg. Chem. Radiochem., 110* (1967) 247.
104 J. P. Lennay, M. Fournier, C. Sanchez, J. Livage and M. T. Pope, *Inorg. Nucl. Chem. Lett., 16* (1980) 257.
105 J. N. Barrows and M. T. Pope, *Adv. Chem. Ser., 226* (1990) 403.